Chapter 3

Experimental Programs for Material Characterization of Hybrid Composites

3.1. Introduction

This chapter deals with the experimental program for mutual characteristics of various composites such as hybrid and functionally graded hybrid composites to be used. Initially, fiber reinforced polymer laminates are prepared by using carbon and glass fibers as primary constituents and epoxy is used as a bonding and matrix agent. Initially plain fiber reinforced polymer specimens are prepared using hand layup process and these specimens are oven cured. All these specimens are checked for different mechanical properties which include tensile, compression , flexural and shear tests. The modulus of elasticity of the fiber specimens are also determined. Later, hybridization of fibers is made by linear gradation of carbon and glass fibers along the thickness direction due to which benefits of both the fibers are utilized. Many strategies have been proposed to make the hybrid more durable and ductile. Utilization of CFRP solely is not economical since carbon fibers are expensive to produce. Alternate hybrid, sandwich hybrid, and functionally graded hybrid specimens have been prepared from carbon and glass fibers. Hand layup technique and oven curing have been used in case of hybrid specimens also. All these specimens are tested for the mechanical properties. Mutual characteristics of the specimens are compared and the layup sequence of the specimen which has better performance is also presented in this chapter. The mechanism implied in such hybrid materials is the sharing of the load applied among the constituents based on its fraction and dispersion. Details of specimen manufacturing test setups and results are explained in the following sections.

3.2. Fabrication of laminates

3.2.1. Plain laminated specimens

Uni-directional carbon and glass fibers were used to prepare laminates and then specimens of required dimensions were made. Carbon fibers had areal density of 50g/m^2 and thickness of 0.19 mm, while the areal density and thickness of glass fabrics is 600g/m^2 and 0.4 mm, respectively. Matrix was prepared by mixing epoxy (resin) of grade 'Resin 691' and hardener of grade 'Reactive Polyamide 140' having 90:10 concentration by weight, respectively. Mechanical properties of resin

and fibers used in this study are given in Table 3.1. Properties of resin such as density, tensile strength, stiffness, failure strain, and thermal decomposition temperature (T_d) are taken from manufacturer, while glass transition temperature of resin was determined using differential scanning calorimetry (DSC) test. Resin was mixed with hardener gently with proper care such that no bubbles were formed in the liquid.

Table 3.1 Mechanical properties of fibers and resin

Property	Dry glass fiber	Dry carbon fiber	Resin*
Density(kg/m^3)	2600	1780	1160
Poisson's ratio	0.30	0.25	0.32
Tensile strength (MPa)	3530	2750	71
Tensile stiffness (GPa)	71	235	3.6
Tensile failure strain (%)	4.5	1.8	4.0
Glass transition temperature, T_g	-	-	91^{o}C
Decomposition temperature, T_d	-	-	230^{o}C

**Grade of resin is T691*

Bubbles result in the formation of voids in the laminate. Hand layup process was used for fabrication of laminates. In this study, volume fraction of fibers in the specimen was limited to 60% (approximately). The fabrication steps are delineated in Fig. 3.1. This method is highly suitable for thermosetting polymer-based composites. Capital and infrastructural requirement is less as compared to other methods. Samples were fabricated by repeatedly stacking the carbon or glass fiber layers with matrix in between layers of fibers. A novel technique is incorporated in this study for uniform pressing of laminates. The thickness of the final laminate depends on the pressure applied. Stacked layers of fibers were first placed in between the aluminum foil (0.75 mm thickness) for good surface finish and ease in demolding as shown in Fig. 3.1(a).

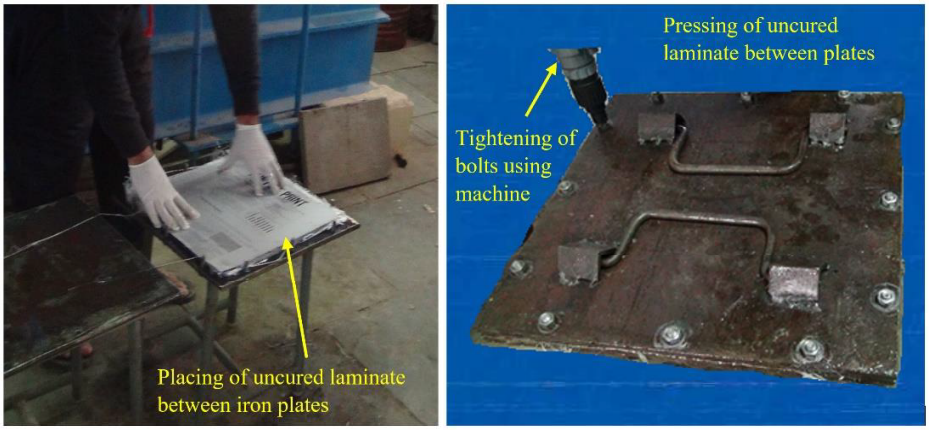

(a) (b)

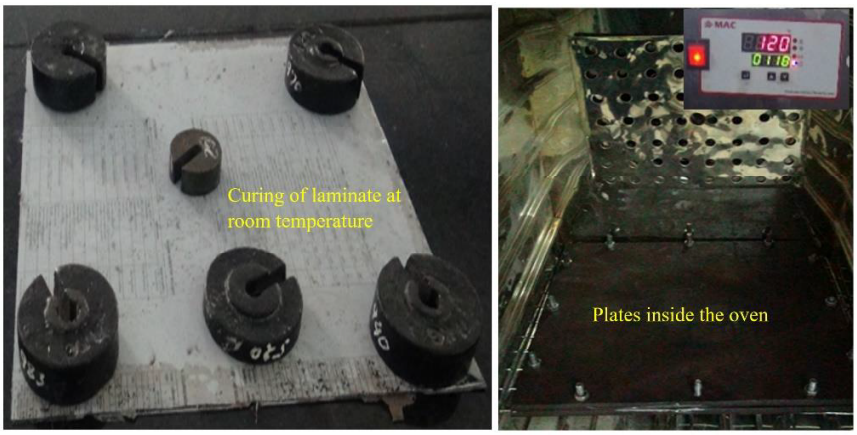

(c) (d)

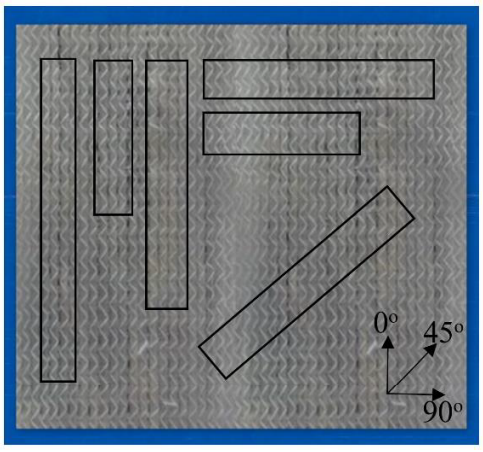

(e)

Fig. 3.1. Fabrication process: (a) Placing the glass fiber-matrix lamina on mild steel plates, (b) Fiber-matrix pressurized between mild steel plates, (c) Open air oven curing, (d) Hot air over curing, (e) Specimens of required dimensions extracted from the laminate.

Further stacked fiber layers in aluminum foil was compressed in between two iron plates of thickness 12 mm each. Iron plates were joined with bolts and each bolt was tightened using bolt tightening machine (torque 250 N-m) as depicted in Fig. 3.1(b). The amount of resin loss by applying the pressure on the uncured laminate was calculated and added to the fiber before placing them between plates.

The percentage of weight loss of resin through sides of laminate increases with the increase in magnitude of pressure and application of time (Thomas *et al.*, 1997). In this process, the extra resin (3% of the total matrix) was added to compensate matrix loss during compression. Later, whole setup was kept at room temperature or cured in hot air oven for a temperature and time (see Fig. 3.1(c) and (d)). Curing of different specimens in hot air oven was carried out at elevated temperatures of 80°C, 120°C and 160°C and for a time span of 1, 2 and 3 hours.

These temperature values were selected based on the lower and higher side of glass transition temperature (91°C) as the glass transition temperature of the resin increases during the elevated temperature curing of the wet resin (Carbas *et al.*, 2014). The room temperature curing of specimens was done for 15 days.

Table 3.2. Description of tensile test specimens

CFRP specimen ID	GFRP specimen ID	Fiber orientation, degree	Temperature of curing, ^{o}C	Time of curing, hour(s)
T0-C-OPN♦	T0-G-OPN	0	27(±3)	360
T0-C80-1♣	T0-G80-1	0	80	1
T0-C80-2	T0-G80-2	0	80	2
T0-C80-3	T0-G80-3	0	80	3
T0-C120-1	T0-G120-1	0	120	1
T0-C120-2	T0-G120-2	0	120	2
T0-C120-3	T0-G120-3	0	120	3
T0-C160-1	T0-G160-1	0	160	1
T0-C160-2	T0-G160-2	0	160	2
T0-C160-3	T0-G160-3	0	160	3
T90-C-OPN	T90-G-OPN	90	27(±3)	360
T90-C80-1	T90-G80-1	90	80	1
T90-C80-2	T90-G80-2	90	80	2
T90-C80-3	T90-G80-3	90	80	3
T90-C120-1	T90-G120-1	90	120	1
T90-C120-2	T90-G120-2	90	120	2
T90-C120-3	T90-G120-3	90	120	3
T90-C160-1	T90-G160-1	90	160	1

T90-C160-2	T90-G160-2	90	160	2
T90-C160-3	T90-G160-3	90	160	3
T45-C-OPN	T45-G-OPN	45	27(±3)	360
T45-C80-1	T45-G80-1	45	80	1
T45-C80-2	T45-G80-2	45	80	2
T45-C80-3	T45-G80-3	45	80	3
T45-C120-1	T45-G120-1	45	120	1
T45-C120-2	T45-G120-2	45	120	2
T45-C120-3	T45-G120-3	45	120	3
T45-C160-1	T45-G160-1	45	160	1
T45-C160-2	T45-G160-2	45	160	2
T45-C160-3	T45-G160-3	45	160	3

♦OPN refers to specimen cured in open air (at room temperature) for 15 days (360 hours)
♣Specimen cured in hot air oven at 80^{o}C temperature for 1 hour

To predict the longitudinal, transverse, and in-plane shear characteristics of laminates, specimens were cut from laminates having fiber orientation of 0°, 90°, and 45° with respect to the longitudinal axis of the specimens as shown in Fig. 3.1(e).

From each laminate, three specimens were cut for a test. Moreover, description of plain FRP specimen ID's of tensile, compression and flexural tests are presented in Tables 3.2–3.4, respectively. The first letter of each specimen ID represents the type of test such as ‘T′ denotes tensile test, ‘C′ denotes compressive test, and ‘F′ denotes flexural test. The numeric term after first letter represents the orientation of fiber with reference to loading, next letter ‘G′ specifies glass fiber, while ‘C′ represents carbon fiber.

Table 3.3 Description of compressive test specimens

CFRP specimen ID	GFRP specimen ID	Fiber orientation, degree	Temperature of curing, ^{o}C	Time of curing, hour(s)
C0-C-OPN♦	C0-G-OPN	0	27(±3)	360
C0-C80-1♣	C0-G80-1	0	80	1
C0-C80-2	C0-G80-2	0	80	2
C0-C80-3	C0-G80-3	0	80	3
C0-C120-1	C0-G120-1	0	120	1
C0-C120-2	C0-G120-2	0	120	2
C0-C120-3	C0-G120-3	0	120	3
C0-C160-1	C0-G160-1	0	160	1
C0-C160-2	C0-G160-2	0	160	2
C0-C160-3	C0-G160-3	0	160	3

C90-C-OPN	C90-G-OPN	90	27(±3)	360
C90-C80-1	C90-G80-1	90	80	1
C90-C80-2	C90-G80-2	90	80	2
C90-C80-3	C90-G80-3	90	80	3
C90-C120-1	C90-G120-1	90	120	1
C90-C120-2	C90-G120-2	90	120	2
C90-C120-3	C90-G120-3	90	120	3
C90-C160-1	C90-G160-1	90	160	1
C90-C160-2	C90-G160-2	90	160	2
C90-C160-3	C90-G160-3	90	160	3

♦ OPN refers to specimen cured in open air (at room temperature) for 15 days (360 hours)
♣Specimen cured in hot air oven at 80°C temperature for 1 hour

The numeric term after 'G′ or 'C′ specify the temperature (°C) at which the specimen was cured, i.e., 80°C, 120°C, 160°C or 27±3°C, i.e., cured at room temperature which is designated as 'OPN'. The last numeric term of specimen ID specifies the time taken for curing, i.e., 1, 2 or 3 h.

3.2.2. Hybrid laminated specimens

The hybrid laminated specimens were also fabricated using hand layup process with carbon and glass fibers as major constituents and epoxy as the matrix for binding purpose. Similar procedure and equal care have been taken in case of hybrid laminated specimens while assembling, curing and machining the specimens of required size. The stacking sequence of hybrid specimens are shown in Fig. 3.2 and the description of specimen ID's are presented in Table 3.5. In specimen ID's, first letters SH, AH or FH represents sandwich, alternate layers of glass-fiber hybrid or functionally graded hybrid specimen, respectively.

After the letters SH, AH or FH, terms 'C' denotes carbon fibers and 'G' denote glass fibers which represent the layer-wise sequence of carbon and glass fibers. For example, in specimen ID SH-$(CCGG)_s$ [Fig. 3.2(c)], after the term 'SH' the letters 'C' and 'G' represents the sequence of carbon and glass fibers, i.e., carbon-carbon-glass-glass fiber laminate, and the subscript 's' denotes laminate is symmetric with respect to the mid-plane.

Table 3.4 Description of flexure test specimens

CFRP specimen ID	GFRP specimen ID	Temperature of curing, ^{o}C	Time of curing, hour(s)
F0-C-OPN♦	F0-G-OPN	27(±3)	360
F0-C80-1♣	F0-G80-1	80	1
F0-C80-2	F0-G80-2	80	2
F0-C80-3	F0-G80-3	80	3
F0-C120-1	F0-G120-1	120	1
F0-C120-2	F0-G120-2	120	2
F0-C120-3	F0-G120-3	120	3
F0-C160-1	F0-G160-1	160	1
F0-C160-2	F0-G160-2	160	2
F0-C160-3	F0-G160-3	160	3

♦ OPN refers to specimen cured in open air (at room temperature) for 15 days (360 hours)
♣Specimen cured in hot air oven at 80^{o}C temperature for 1 hour

Fig. 3.2 shows the functionally graded hybrid specimen FH-(GC)s-I, where 'GC' represents glass fibers are functionally graded around carbon fibers. In this specimen, the first layer (from top) has 100% glass fibers, while in the second layer 25% carbon fibers are in middle and 37.5% glass fibers are on each side. The third layer has 75% carbon fibers in middle and 12.5% glass fibers on its each side and other layers are symmetrical with respect to the reference plane which is in the middle and the fourth layer has completely carbon fibers. Layers are symmetrical about the reference plane which is in between the fourth and fifth layer. In short, glass fibers are functionally graded about carbon fibers in FH-$(CG)_s$-I variation of glass fibers is 0%, 25%, 75%, and 100% of the width of the specimen as shown in Fig. 3.2(j). The percentage of variation of fibers can be represented by (0/25/75/100) and in specimen ID's, this layup is denoted as 'I'. Similarly, the type 'II' and 'III' of functionally graded hybrid specimens are (0/33/67/100) and (0/50/50/100), respectively. In the similar way, FH-(CG)s-I specimen ID's represents carbon fibers are functionally graded around the glass fibers.

Table 3.5 Description of laminates.

Laminate type	Tensile test specimen ID	Compressive test specimen ID	Flexure test specimen ID
Plain CFRP	T-$(CCCC)_s$ ♦	C-$(CCCC)_s$ ♠	F-$(CCCC)_s$ ♥
Plain GFRP	T-$(GGGG)_S$	C-$(GGGG)_s$	F-$(CCCC)_s$
Sandwich hybrid	T-SH-$(CCGG)_s$	C-SH-$(CCGG)_s$	F-SH-$(CCGG)_s$
Sandwich hybrid	T-SH-$(GGCC)_s$	C-SH-$(GGCC)_s$	F-SH-$(GGCC)_s$
Alternate hybrid	T-AH-$(CGCG)_s$	C-AH-$(CGCG)_s$	F-AH-$(CGCG)_s$
Alternate hybrid	T-AH-$(GCGC)_s$	C-AH-$(GCGC)_s$	F-AH-$(GCGC)_s$
Functionally graded hybrid	T-FH-$(CG)_s$-I	C-FH-$(CG)_s$-I	F-FH-$(CG)_s$-I
Functionally graded hybrid	T-FH-$(CG)_S$-II	C-FH-$(CG)_s$-II	F-FH-$(CG)_s$-II
Functionally graded hybrid	T-FH-$(CG)_s$ -III	C-FH-$(CG)_s$ -III	F-FH-$(CG)_s$ - III
Functionally graded hybrid	T-FH-$(GC)_s$-I	C-FH-$(GC)_s$-I	F-FH-$(GC)_s$-I
Functionally graded hybrid	T-FH-$(GC)_s$-II	C-FH-$(GC)_s$-II	F-FH-$(GC)_s$-II
Functionally graded hybrid	T-FH-$(GC)_s$-III	C-FH-$(GC)_s$-III	F-FH-$(GC)_s$-III

♦'T' stands for tensile test, ♠'C' stands for Compressive test, ♥'F' stands for Flexure test
'I' represents layup sequence $(0/25/75/100)_s$, 'II' denotes layup sequence $(0/33/66/100)_s$ & 'III' represents layup sequence $(0/0/50/100)_s$

3.3. Experimental tests

The main objective of the tests is to determine the mechanical characteristics of FRP laminated specimens cured at various temperatures for different durations.

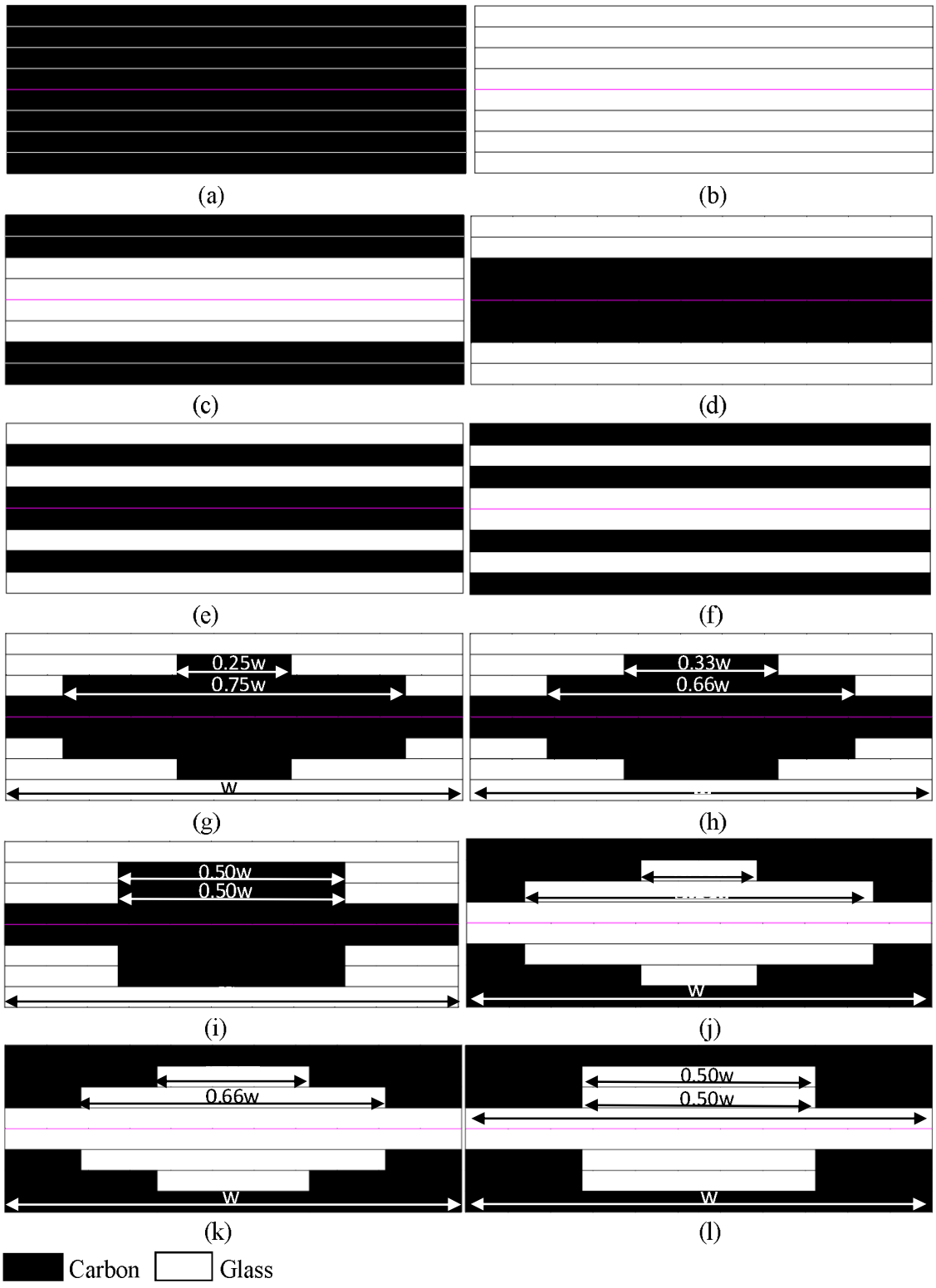

Fig. 3.2. Layup sequence of sandwich hybrid, alternate layer hybrid, and functionally graded hybrid specimens in thickness direction: **(a)** $(CCCC)_s$; **(b)** $(GGGG)_s$; **(c)** SH-$(CCGG)_s$; **(d)** SH-

$(GGCC)_s$; **(e)** AH-$(GCGC)_s$; **(f)** AH-$(CGCG)_s$; **(g)** FH-$(GC)_s$-I; **(h)** FH-$(GC)_s$-II; **(i)** FH-$(GC)_s$-III; **(j)** FH-$(CG)_s$-I; **(k)** FH-$(CG)_s$-II; **(l)** FH-$(CG)_s$-III

Effect of temperature and curing time on the change in the strength and stiffness of CFRP and GFRP laminates was evaluated under tension, compression and flexural loading. Performance of laminates was determined by conducting the tests on the flat specimens. Even though, there are different test methods to determine the mechanical parameters, but ASTM standards (ASTM E1356-08, 2014; ASTM D3039/D3039M, 2013; ASTM D3410, 2000; ASTM D790, 2002) were considered in this study to determine the behavior of the FRP laminated specimens under different loadings. Description of each test setup is described in the following sections. Five number of samples for each test for a particular scenario is considered.

3.3.1 Glass transition temperature test

The glass transition temperature of the resin was determined as per the standard specifications (ASTM E1356-08, 2014). A strip of neat epoxy (thickness 0.5 mm) was prepared at room temperature and three samples were cut (diameter 3 mm) and weighing 6 mg each. These samples were placed in the aluminum pans as shown in Fig. 3.3(a) and tested using differential scanning calorimetry (DSC) apparatus as shown in Fig. 3.3(b). In this test, samples were placed in the heating chamber at a rate of 10 °C/min and test was started at room temperature of 26.4 °C. The averaged glass transition temperature of resin is calculated as 91.23 °C.

3.3.2. Tensile test

Tensile characteristics such as tensile strength and stiffness were determined by testing of CFRP and GFRP specimens as per the guidelines (ASTM D3039/D3039M, 2013). Tests were conducted in universal testing machine (UTM) of 100 kN capacity which was preinstalled in the structural laboratory, BITS Pilani. The specimens were gripped in between the wedge grips such that entire grip length covers the face of the grips. The pressure in the wedge grips was adjusted to prevent the specimen from slippage and failure at grips during tension. The hydraulic grip pressure for holding the specimen was maintained at 3.5 MPa. At this pressure, slippage or breakage of specimens inside the grips were not observed. The rate of displacement of the crosshead was 2 mm/min. Specimens were machined from the fabricated laminates as per the dimensions specified in code (ASTM D3039/D3039M, 2013).

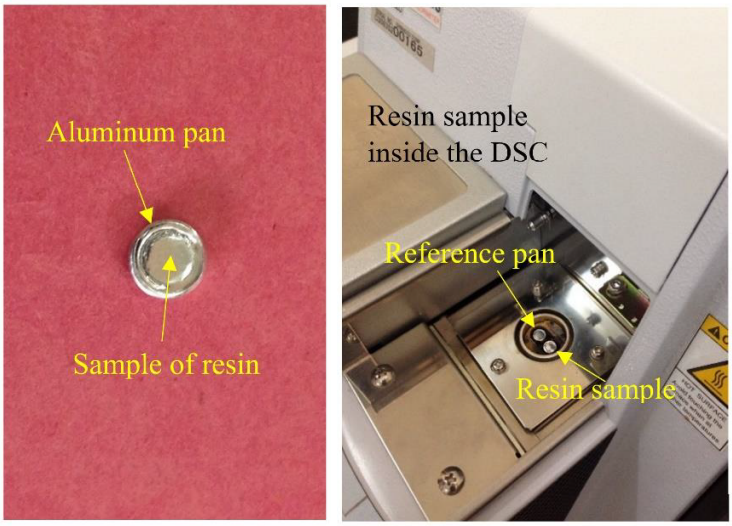

(a) (b)

Fig. 3.3. Glass transition temperature of the resin evaluated using Differential Scanning Calorimetry (DSC): (a) Resin sample used for testing, (b) Sample tested inside DSC.

The dimensions of specimens having fiber orientation 0°, i.e., parallel to loading direction was 250×15×1.2±(0.15–0.35) mm (length × width× thickness); dimensions for specimens having fibers perpendicular to the loading direction, i.e., fibers oriented at 90° was 175 × 25 × 1.2±(0.15–0.35) mm (length × width × thickness), and for the specimens having fiber orientation 45° inclined to the loading direction was 190 × 25 × 1.2±(0.15–0.35) mm (length × width × thickness). In each specimen, grip length was 50 mm on both ends, while the gage length was kept 150, 90 and 75 mm for specimens having fiber orientation 0°, 45° and 90°, respectively with respect to loading direction.

3.3.2.1. Energy absorbed

Total energy absorbed by the material was determined by calculating the area under the load-deflection curve till the point of ultimate failure, which represents the strain energy or elastic energy absorbed (Singh and Chawla, 2016). Moreover, the non-linearity is associated with the plastic flow in the specimen. Behavior of the material, whether it is ductile, or brittle is predicted based on the amount of elastic and plastic energy absorbed. However, brittle materials are typically linear till the end and finally end up with a fracture without any plastic flow. Total energy absorbed is calculated by integrating the load-deflection curve, considering the limits zero to the maximum displacement at which the specimen fails. In this study, trapezoidal rule was applied to find out the

area under theload vs displacement curve using Eq. (1). The trapezoidal rule can be applied directly to the data available and area was calculated accordingly.

$$A = \int_{a}^{b} f(x).dx = \sum_{k=1}^{N} \frac{f(x_{k-1}) + f(x_k)}{2} \Delta x_k \quad (1)$$

where, A is the area under the curve, 'a' is the initial point of the curve, 'b' is the end point of the curve, 'k' is the interval, 'N' is the total number of intervals, and Δx_k is the width of each sub-interval. The proportional limit in the stress-strain curve is the elastic limit and beyond elastic limit was considered as plastic deformation which is irreversible. Further, the elastic energy was calculated by the area under the linear region in the load vs deflection curve. This represents the amount of elastic flow in the specimen. The elastic slope was calculated from the Eq. (2).

$$S = \frac{P_1 S_1 + (P_2 - P_1) S_2}{P_2} \quad (2)$$

where, S is the slope of elastic region, S_1 is the slope of the first linear portion, S_2 is slope of the second linear portion, P_1 is maximum load of the first linear portion and P_2 is maximum load of second linear portion. Further, inelastic energy was calculated by deducting the elastic energy from total energy determined.

3.3.2.2. Shear modulus

In this study, shear modulus was predicted from the uniaxial tensile test of 45° fiber aligned FRP and GFRP specimens. When the specimen was tested in the tensile mode, the shear failure occurred in the direction of 45° to the x-axis. In this case, shear modulus was determined using Eq. (3).

$$G_{12} = \frac{1}{\frac{4}{E_x} - \frac{1}{E_1} - \frac{1}{E_2} + \frac{2\upsilon_{12}}{E_1}} \quad (3)$$

where, G_{12} is the shear modulus; E_x is the modulus of elasticity of specimen in the loading direction (determined from first linear slope of stress-strain curve of 45° specimens), E_1 is the longitudinal Young's modulus in fiber direction, E_2 is the transverse Young's modulus in transverse to the fiber direction and υ_{12} is the Poisson's ratio of the laminate in plane of 1-2, where direction '1' refers to the fiber direction.

3.3.3. Compressive test

Compressive strength and failure strain were determined using the ASTM standards (ASTM D3410, 2000). Dimensions of the 0° unidirectional fiber orientation specimens were 105 x 10 x 1.2±(0.15-0.35) mm (length x width x thickness) while for 90° fiber oriented specimens, dimensions were 105 x 25 x 1.2±(0.15-0.35) mm (length x width x thickness). For specimens of 0^o and 90° fiber aligned, gage and grip lengths were taken same, i.e., 25 mm and 40 mm, respectively. Specimens were tested using universal testing machine of 100 kN capacity at displacement rate of 1.5 mm/min. In order to prevent the slippage or breakage of specimen inside grips, hydraulic grip pressure for holding the specimen was maintained at 3.5 MPa. Mode of failure, and its location was noted.

3.3.4. Flexural test

Flexural characteristics of specimens were determined using the ASTM standards (ASTM D790-02, 2002). All the specimens had fiber orientation along the length of specimen, i.e., 0° and the dimensions of each specimens were 160 x 25 x 1.2±(0.15-0.35) mm (length x width x thickness). Span length of 80 mm and overhang of 40 mm on each side of specimen was considered. Self-fabricated supports (6 mm diameter) and loading nose (12 mm diameter) were used in this test. Rate of crosshead motion (R) was calculated from Eq. (4) and was determined as 0.11 mm/s.

$$R = \frac{ZL^2}{6d} \tag{4}$$

where, L is support span (mm), d is depth (mm) of specimen and Z is rate of straining of the outer fiber (mm/mm/min). As per the code, strain (Z) is taken as 0.01. Tests were performed till the complete failure of specimens. The flexural strength (σ) of specimens was determined by Eq. 5.

$$\sigma = \frac{3PL}{2bd^2} \tag{5}$$

where, P is the maximum load (N) applied at mid-span of the specimen, and b is width (mm) of beam tested.-The flexural modulus (E) obtained from three-point bending test of specimen was calculated using Eq. (6).

$$E = \frac{L^3 m}{4bd^2} \tag{6}$$

where, *m* is the slope of the tangent determined from the initial straight-line portion of the load-deflection curve (N/mm). Coefficient of variation (*CV*) was measured for every set of specimens tested in laboratories to verify precision and reliability. Flexural strain depends on the fractional change in the length of the specimen when the load was applied at the midspan. The flexural strain (ε) of the fiber reinforced polymer specimens was determined from Eq. (7).

$$\varepsilon = \frac{6Dd}{L^2} \tag{7}$$

where, *D* is the maximum deflection of beam (mm) occurring at midspan. Further the results and failure characteristics of each specimen are discussed in the following sections.

The interface in laminated composites plays a vital role in characterizing the behavior of laminated composite materials since they are responsible for displacements and tractions across the interlaminar interface. Scanning electron microscope (SEM) analysis has been conducted on the functionally graded hybrid specimen to show the interfacial bond between the adjacent layers and is depicted in Fig. 3.4

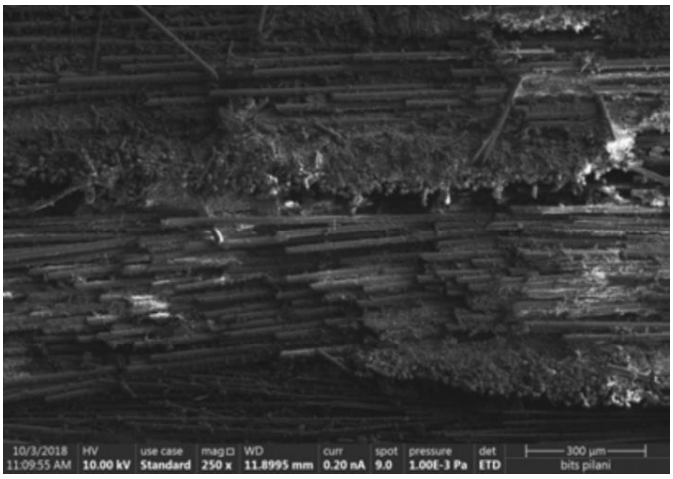

Fig. 3.4. SEM image showing interface in carbon/glass FH laminate

3.4. Results and Discussion

In this section, the tensile, compressive, in-plane shear and flexural characteristics of different CFRP and GFRP specimens cured for different temperatures are compared with that of specimens cured at room temperature. Also, the effect of linearly graded glass and carbon fibers on tensile,

compressive, and flexural characteristics of laminates are investigated as well as its properties are compared with that of sandwich, alternate, and functionally graded hybrid laminates

In order to facilitate the comparison of strength, stiffness and failure strains, bar charts are made individually for the CFRP and GFRP specimens cured at different temperatures for different durations. Moreover, percentage difference in the characteristics of temperature cured specimens with respect to the room temperature cured specimens is determined and presented in bar charts. In addition, accuracy of measured characteristics of each test are described in terms of coefficient of variation.

Failure mode of each specimen is presented. Comparison of strength, stiffness and failure strain of each hybrid and non-hybrid specimens are presented in the bar charts, which is helpful in finding out the advantages and disadvantages of functionally graded carbon/glass fiber laminate. The percentage values written on the bottom of bars of each hybrid specimen represents the hybrid effect which means difference in magnitude of the specimen with respect to CFRP or GFRP specimens. Failure strains are calculated at the point, where 30% drop in load occurs in the specimen. The detailed discussion on the behavior of laminates under tensile, compressive, and flexural loading is explained further.

3.4.1. Tensile characteristics

3.4.1.1 CFRP laminates

The mode of failure observed in tensile CFRP specimens was splitting gage middle failure as shown in Fig. 3.5(a), which indicates that the specimen fails by splitting of fibers in its gage length with considerable damage to the specimen. In this study, it is observed that CFRP specimens (T0-C80-3) cured at 80^{o}C for three hours have higher tensile strength (Fig. 3.5(b)) and stiffness (Fig. 3.5(c)) with respect to the other temperature cured specimens. In the Figures, percentage values (positive/negative) above each bar represents the percentage increase or decrease in the corresponding strength/modulus or failure strain with respect to that of specimen cured at room temperature while the values at bottom of bars in the Figures represent the coefficient of variation in the properties. It is worth noting that strength and stiffness of specimens increases with increase in the duration of curing, specifically at the temperatures 80^{o}C and 120^{o}C. Fig. 3.5(d) shows that curing temperature has significant effect on the failure strain of composites. Like strength and stiffness, failure strain of specimen T0-C160-1 is equivalent to tensile characteristics of specimen

cured at room temperature. It is concluded that, in order to achieve early curing, CFRP specimens have to be cured at temperature of 160ºC for 1-hour which gives better strength, stiffness and failure strain; and equivalent to the specimens cured at room temperature for 15 days.

(a)

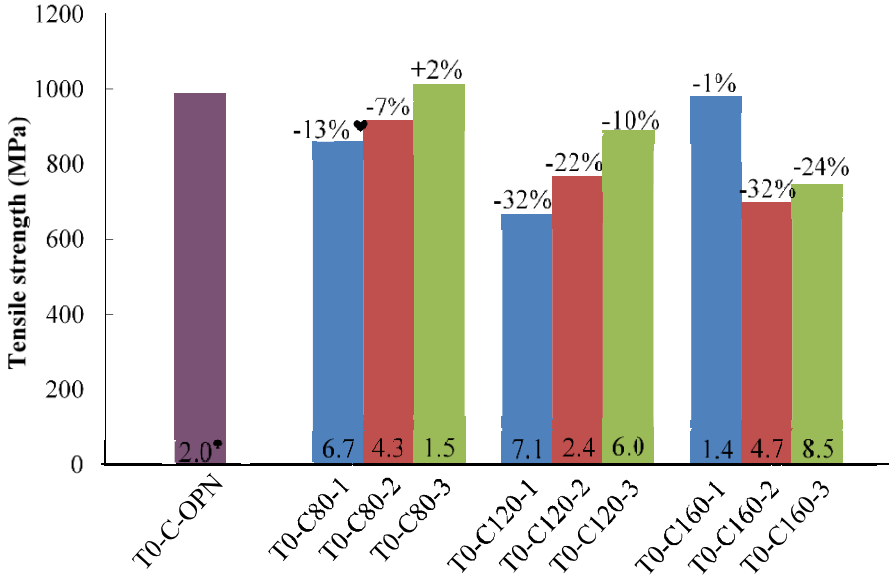

♠Coefficient of variation, ♥Variation w.r.t room temperature cured specimen (T0-C-OPN).

(b)

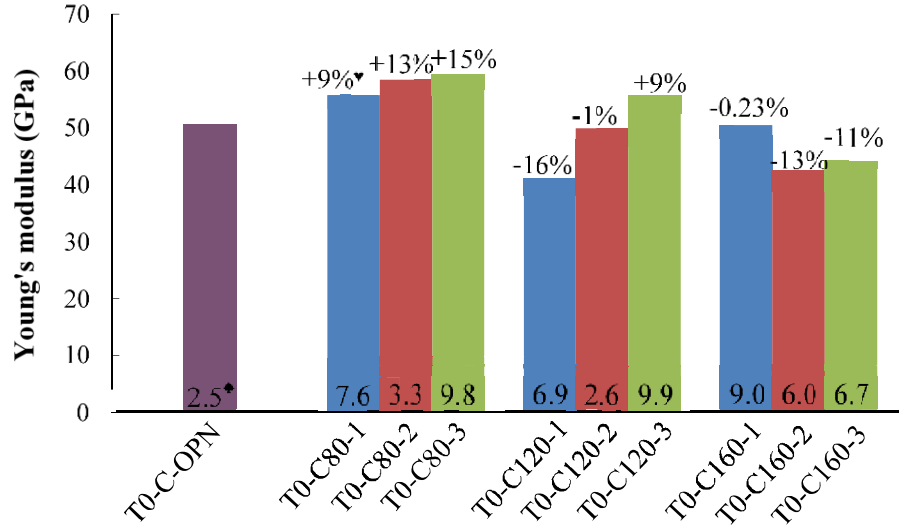

♠Coefficient of variation, ♥Variation w.r.t room temperature cured specimen (T0-C-OPN).

(c)

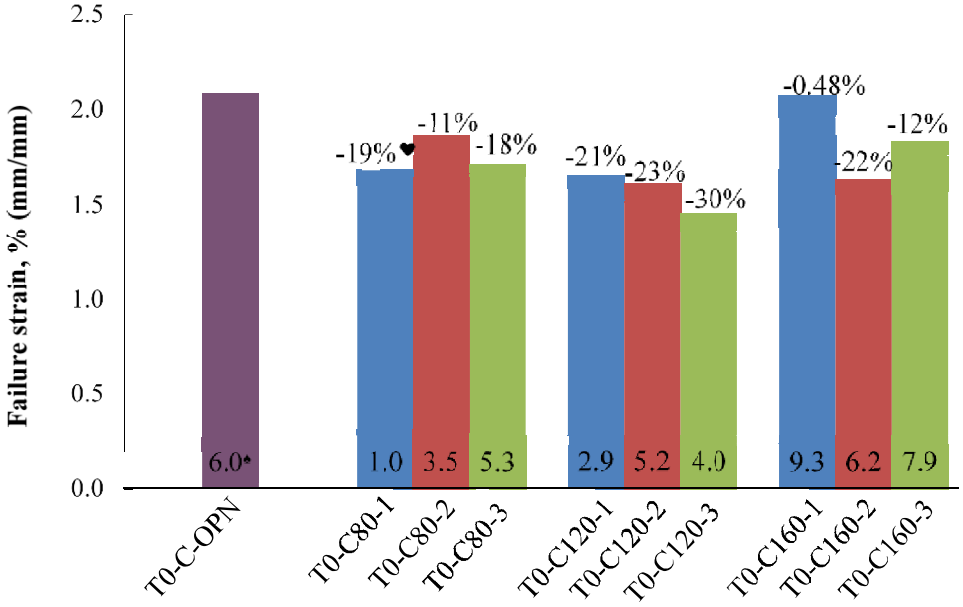

♠Coefficient of variation, ♥Variation w.r.t. room temperature cured specimen (T0-C-OPN).

(d)

Fig. 3.5. Tensile test results of 0^{o} fiber aligned CFRP specimens: (a) Failure mode, (b) Tensile strength, (c) Young's modulus, (d) Failure strain.

In case of 90^{o} fiber aligned CFRP specimens, the type of failure observed was lateral gage middle (LGM) failure, appeared in the gage length of the specimen as shown in Fig. 3.6(a). Tensile

strength of all 90º fiber aligned CFRP specimens is presented in Fig. 3.6(b) while tensile modulus is presented in Fig. 3.6(c). Fig. 3.6(b) shows that specimen T90-C160-2 cured at 160ºC for two hours has almost same tensile strength as the specimens cured at room temperature for 15 days. It is worth mentioning that specimens cured for two hours have higher transverse strength than those cured for 1 and 3 hours. Tensile stiffness of specimen T90-C80-1 is higher than all other specimens. Moreover, all other specimens have lesser stiffness than specimen cured at room temperature. From Fig. 3.6(d), it is noticed that specimens other than T90-C80-1 and T90-C80-2, have higher failure strain than room temperature cured specimen. Even though, specimen T90-C80-1 has higher stiffness than other specimens, its failure strain is lower. Specimens cured at temperature of 160ºC for 1 and 3 hours have shown significant rise in failure strain with respect to the room temperature cured specimens.

(a)

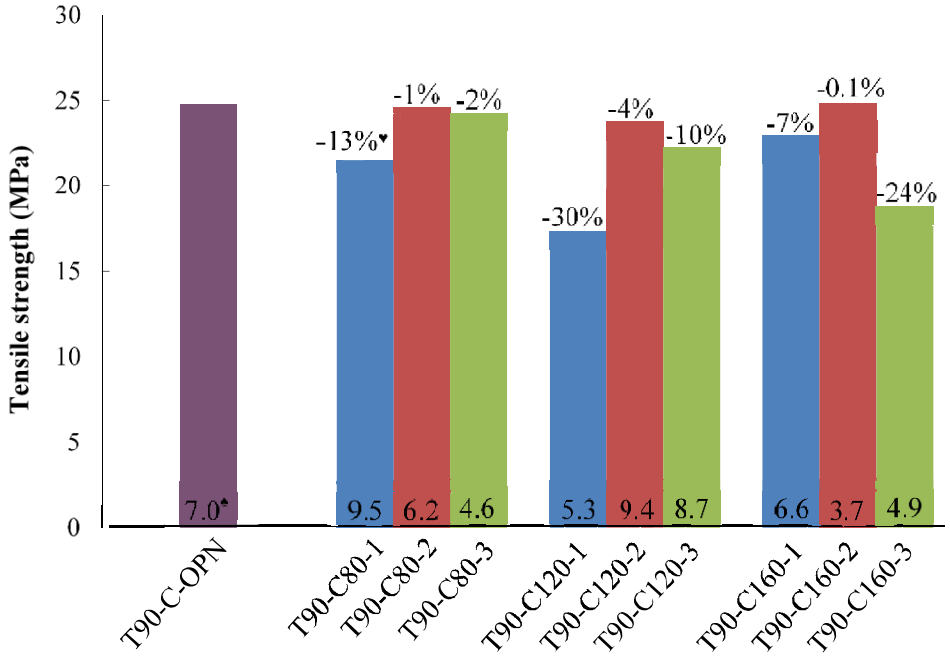

♠Coefficient of variation, ♥Variation w.r.t. room temperature cured specimen (T90-C-OPN).

(b)

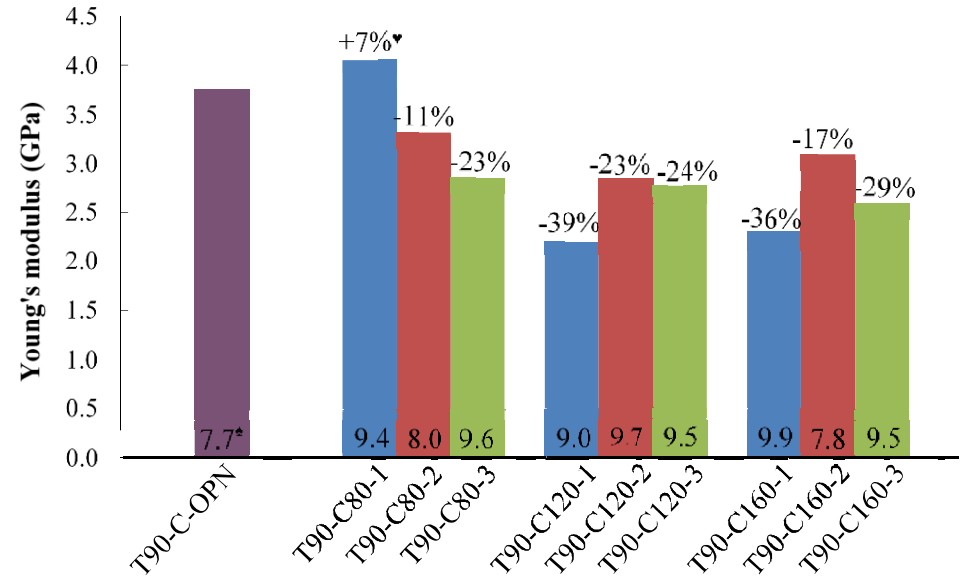

♠Coefficient of variation, ♥Variation w.r.t room temperature cured specimen (T90-C-OPN).

(c)

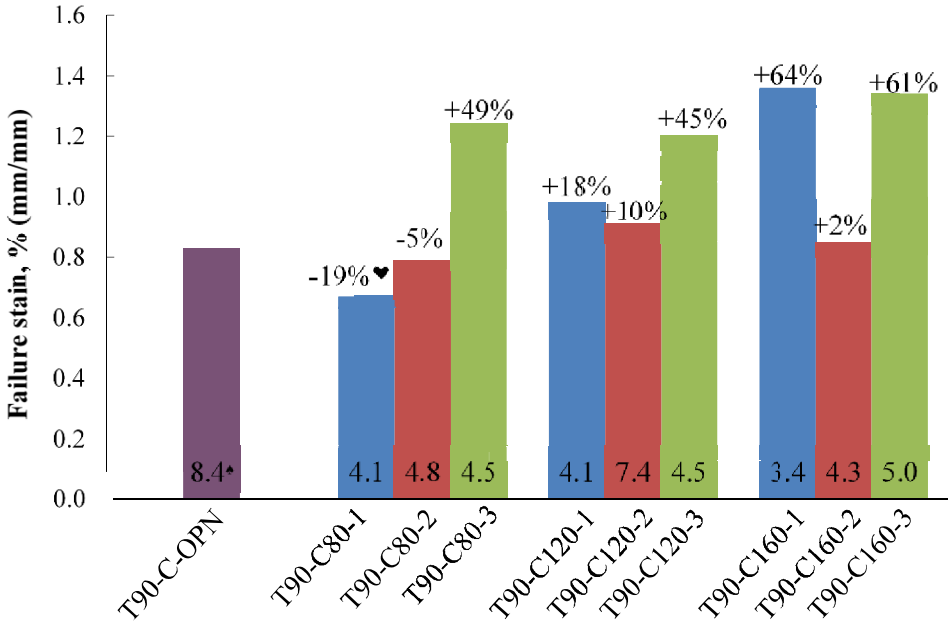

♠Coefficient of variation, ♥Variation w.r.t. room temperature cured specimen (T90-C-OPN).

(d)

Fig. 3.6. Tensile test results of 90^o fiber aligned CFRP specimens: (a) Failure mode, (b) Tensile strength, (c) Young's modulus, (d) Failure strain.

For more clarity of the positive effect of temperature curing, normalization curves are plotted in Fig. 3.7 for CFRP specimens to show the relationship between ratios of the properties obtained at elevated temperature (80^{o}C, 120^{o}C, 160^{o}C) curing to that of room temperature curing versus duration of curing in hours. The ratio of tensile strength of the 0^o fiber aligned specimens cured at a specific temperature (T_t) to the specimens cured at room temperature (T_o) are shown in Fig. 3.7(a).

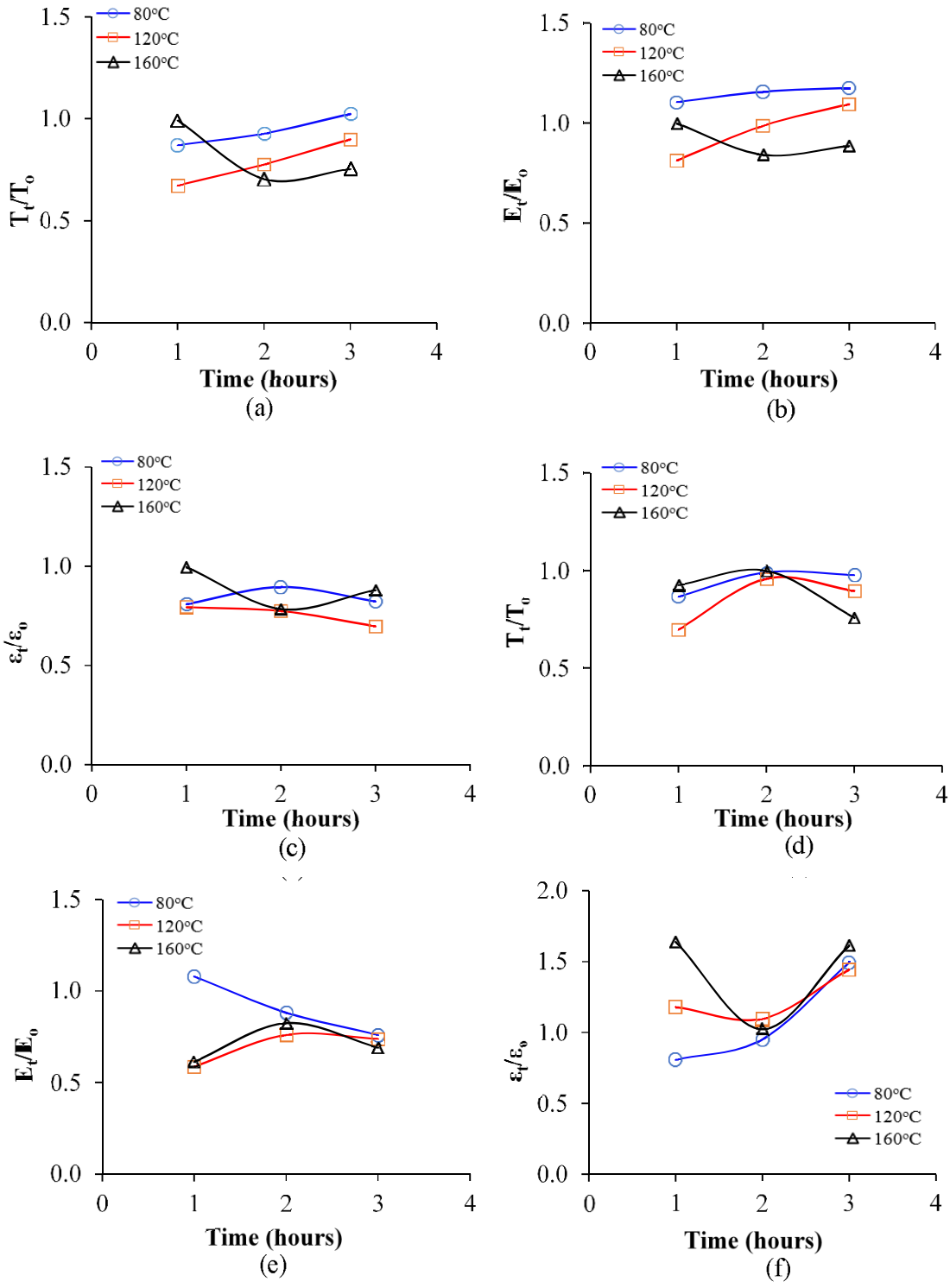

Fig. 3.7. Normalized curves of tensile characteristics of CFRP: (a) Tensile strength of specimen in 0^o fiber direction, (b) Youngs modulus of elasticity of specimen in 0^o fiber direction, (c) Failure strain of specimen in 0^o fiber direction, (d) Tensile strength of specimen in 90^o fiber direction, (e)

Youngs modulus of elasticity of specimen in 90^o fiber direction, (f) Failure strain of specimen in 90^o fiber direction.

Similarly, Figs. 3.7(b) and 3.7(c) represent the Young's modulus of elasticity and failure strain, respectively of the 0^o fiber aligned tensile specimens. The tensile characteristics such as tensile strength, modulus of elasticity and failure strain of 90^o fiber aligned specimens are shown in Figs. 3.7(d), 3.7(e), and 3.7(f), respectively.

3.4.1.2 GFRP laminates

The failure mode observed in GFRP specimens having fiber orientation 0^o was splitting gage middle (SGM) failure, which occurred by splitting of fibers in the gage length of the specimen as shown in Fig. 3.8(a). Tensile strength variations are represented in the form of bar chart as shown in Fig. 3.8(b), while tensile modulus of specimens is presented in Fig. 3.8(c). It is observed that a FRP specimen T0-G80-3 cured at 80^{o}C for three hours attained the maximum tensile strength amongst all 0^o fiber aligned GFRP tensile specimens, and it is 18% higher than the T0-G-OPN specimen. High tensile stiffness (Fig. 3.8(c)) was achieved in the T0-G120-3 specimen, which is 11% higher than room temperature cured specimen. Significant rise in Young's modulus of the longitudinal fiber oriented GFRP specimens is observed in this study, in contrast to the Young's modulus obtained by Achintha and Balan, 2017, calculated through finite element analysis. From Fig. 3.8(d), it is observed that specimens cured at elevated temperature shows higher failure strain than room temperature cured specimens. It is worth noting that specimen T0-G80-2 has shown significantly high failure strain in comparison with open air cured specimens.

(a)

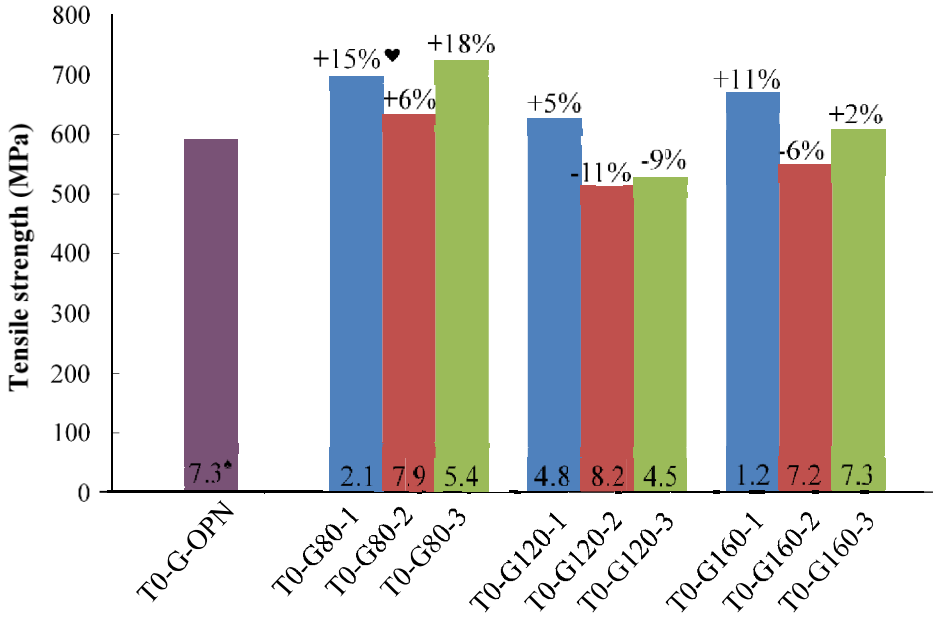

♠Coefficient of variation, ♥Variation w.r.t. room temperature cured specimen (T0-G-OPN).

(b)

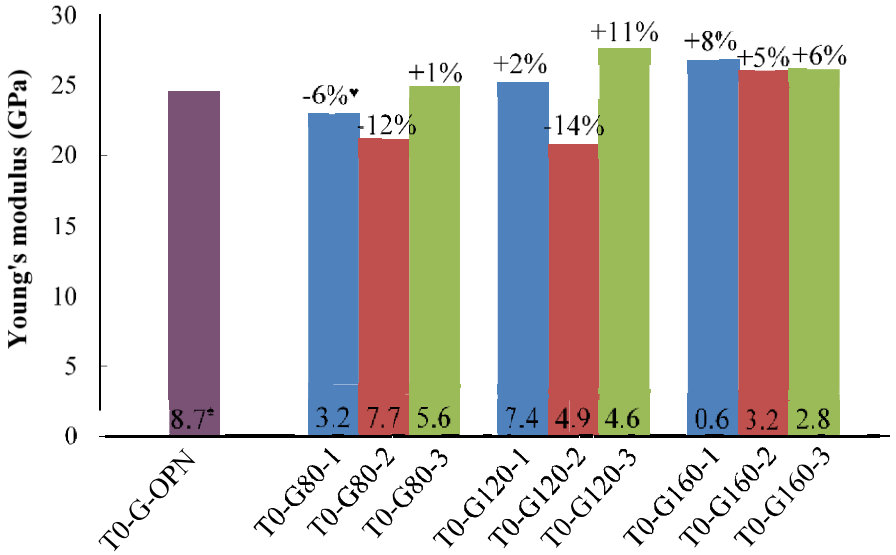

♠Coefficient of variation, ♥Variation w.r.t. room temperature cured specimen (T0-G-OPN).

(c)

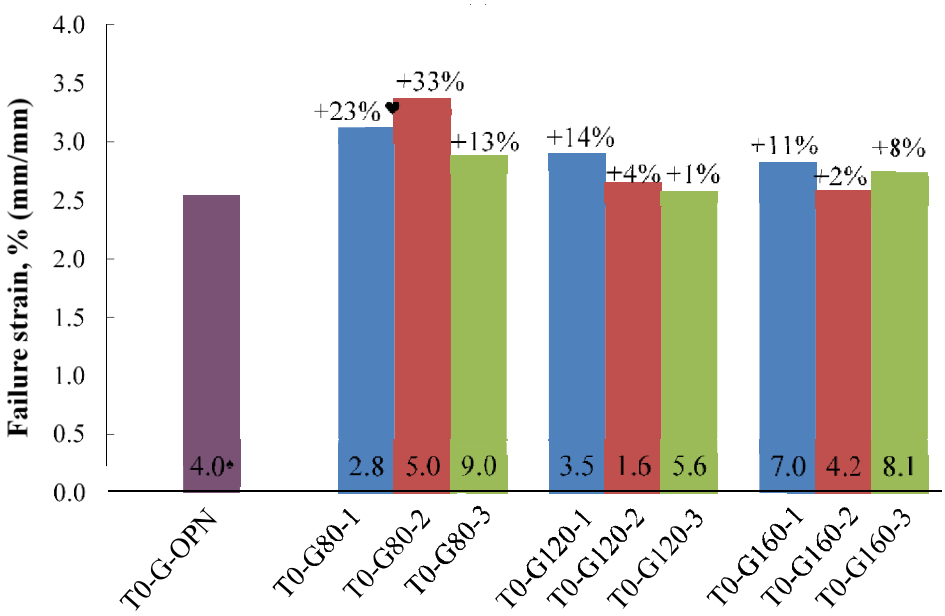

♠Coefficient of variation, ♥Variation w.r.t. room temperature cured specimen (T0-G-OPN).

(d)

Fig. 3.8. Tensile test results of 0° fiber aligned GFRP specimens: (a) Failure mode, (b) Tensile strength, (c) Young's modulus, (d) Failure strain.

In case of 90° fiber aligned GFRP specimens, the type of failure observed was lateral gage middle (LGM) failure, occurred in the gage length of the specimen as depicted in Fig. 3.9(a). These specimens failed laterally, i.e., transverse to the fiber direction in the gage length of the specimen in a catastrophic manner. Like longitudinal tensile strength of GFRP laminate, the maximum transverse tensile strength was also observed in laminate which is cured at temperature of 80°C for three hours, i.e., T90-G80-3 (see Fig. 3.9(b)). Tensile strength is approximately 8% higher than the specimens cured at room temperature. From Fig. 3.9(b), it is noted that out of all 120°C and 160°C temperature cured specimens, T90-G120-3 and T90-G160-3 specimens achieved maximum tensile strengths, respectively. Moreover, maximum Young's modulus in the 90° fiber aligned specimens was achieved at temperature of 160°C for three hours curing as shown in Fig. 3.9(c). Fig. 3.9(d) depicts that specimens T90-G80-3 and T90-G120-1 exhibited highest failure strain amongst all specimens. It is worth noting that laminate cured at temperature of 80°C for three hours achieved the higher longitudinal and transverse tensile strength, along with longitudinal and transverse Young's modulus, and failure strain than specimens cured at room temperature. Hence,

curing of GFRP laminates at temperature of 80°C for three hours is recommended for applications where tensile stresses are dominant.

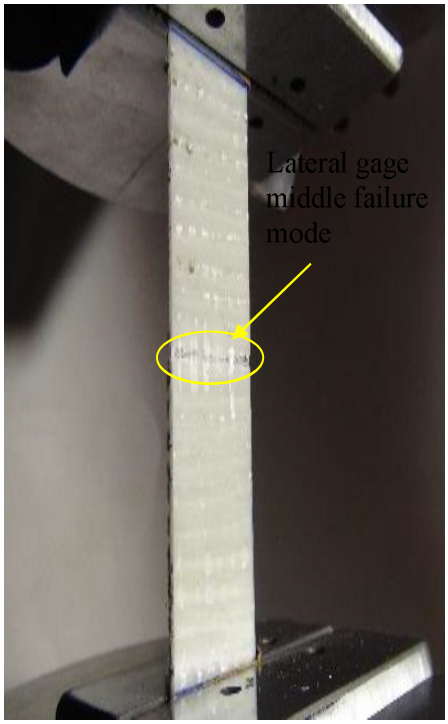

(a)

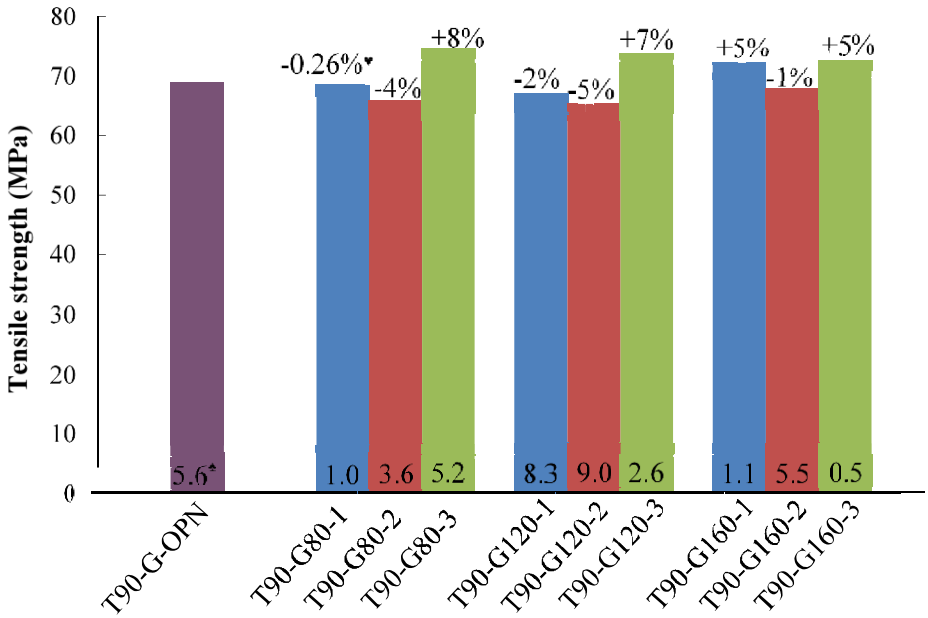

♠Coefficient of variation, ♥Variation w.r.t. room temperature cured specimen (T90-G-OPN).

(b)

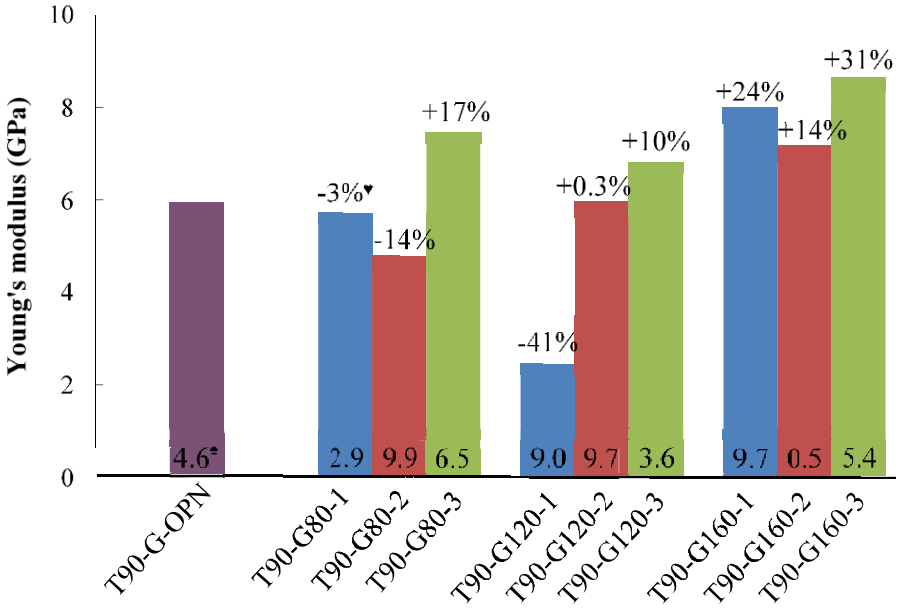

♠Coefficient of variation, ♥Variation w.r.t room temperature cured specimen (T90-G-OPN).

(c)

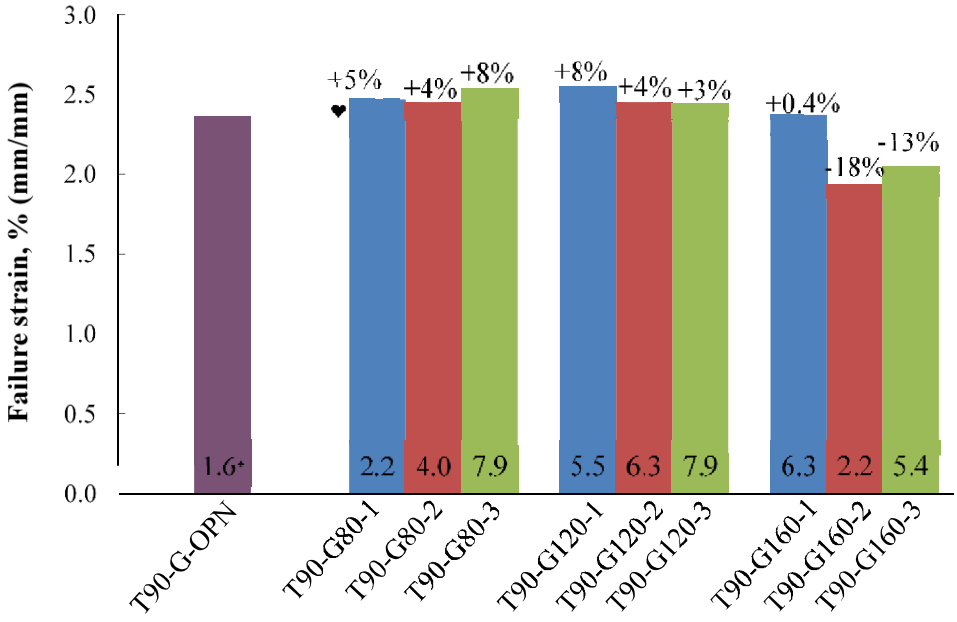

♠Coefficient of variation, ♥Variation w.r.t. room temperature cured specimen (T90-G-OPN).

(d)

Fig. 3.9. Tensile test results of 90^{o} fiber aligned GFRP specimens: (a) Failure mode, (b) Tensile strength, (c) Young's modulus, (d) Failure strain.

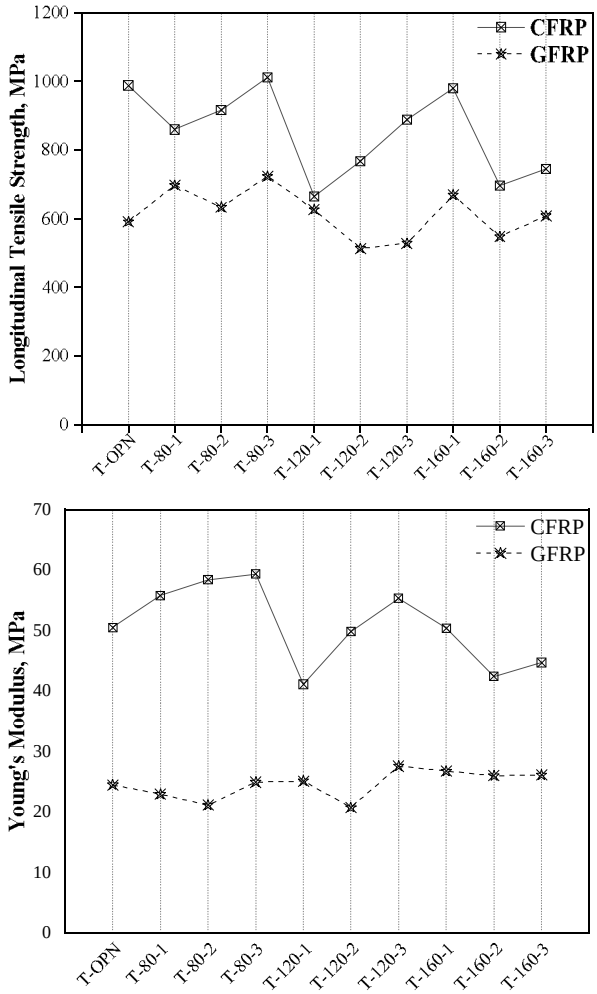

(a) (b)

Fig. 3.10. Variation in curing experimental (a) longitudinal strength and (b) Young's Modulus between CFRP and GFRP specimens

Figures 3.10 (a) and 3.10 (b) depict the variance in longitudinal tensile strength and Young's modulus of elasticity between CFRP and GFRP at various curing temperatures. In all circumstances, CFRP outperforms GFRP in terms of tensile strength and modulus of elasticity. Specimens cured at 80°C for 3 hours in both CFRP and GFRP show maximal tensile strength, as illustrated in Fig. 3.10. (a). CFRP specimens have a high modulus of elasticity when cured at 80°C for 3 hours, but GFRP specimens require 120°C for 3 hours.

For the sake of clarity of the positive effect of temperature curing, normalization curves are plotted in Fig. 3.10 to show the relationship between the ratios of properties of elevated temperature cured and room temperature cured specimens with respect to the duration of curing. Figs. 3.10(a),

3.10(b), and 3.10(c) denote the tensile strength, modulus of elasticity, and failure strain of 0° fiber aligned GFRP specimens. Strength, modulus of elasticity, and failure strain of GFRP specimens aligned in transverse direction are outlined in Figs. 3.10(d), 3.10(e), and 3.10(f), respectively.

3.4.1.3. Energy absorbed

The total energy absorbed in tensile specimens of CFRP and GFRP laminates is determined using Eq. (1), while the elastic energy is determined using Eq. (2). In 0° fiber aligned CFRP specimens, elastic energy of most of the specimens are enormous compared to inelastic energy attained as shown in Fig. 3.12(a).

Temperature and cure time have been found to have a substantial impact on the amount of energy absorbed in laminates. In comparison to other specimens, CFRP laminates cured at 80°C for 1 hour exhibit the largest inelastic energy absorptions. It is observed that, as duration of curing increases for 80°C temperature cured specimens, the elastic and inelastic energies increase and decrease, respectively. In case of 90° fiber aligned CFRP specimens (see Fig. 3.12(b)), both elastic energy and inelastic energy increases as duration of curing time increases. Elastic energy in the specimens cured at room temperature is higher than the 80°C temperature cured specimen for 1-hour duration. Remaining specimens are dominant when compared with room temperature cured specimens (see Fig. 3.12(b)). Since the transverse strength of CFRP specimens is low, elastic and inelastic energies of 90° CFRP specimens are lower than CFRP 0° fibers aligned specimens.

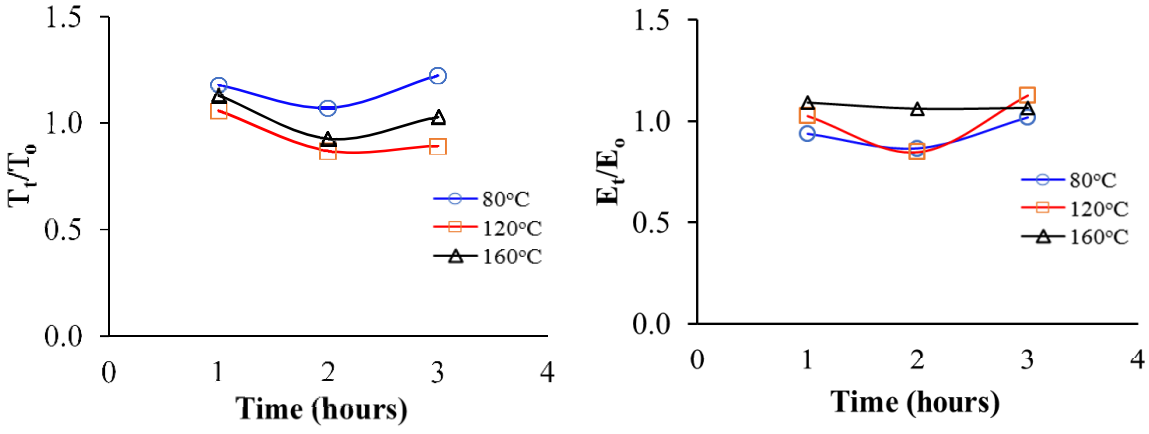

(a) (b)

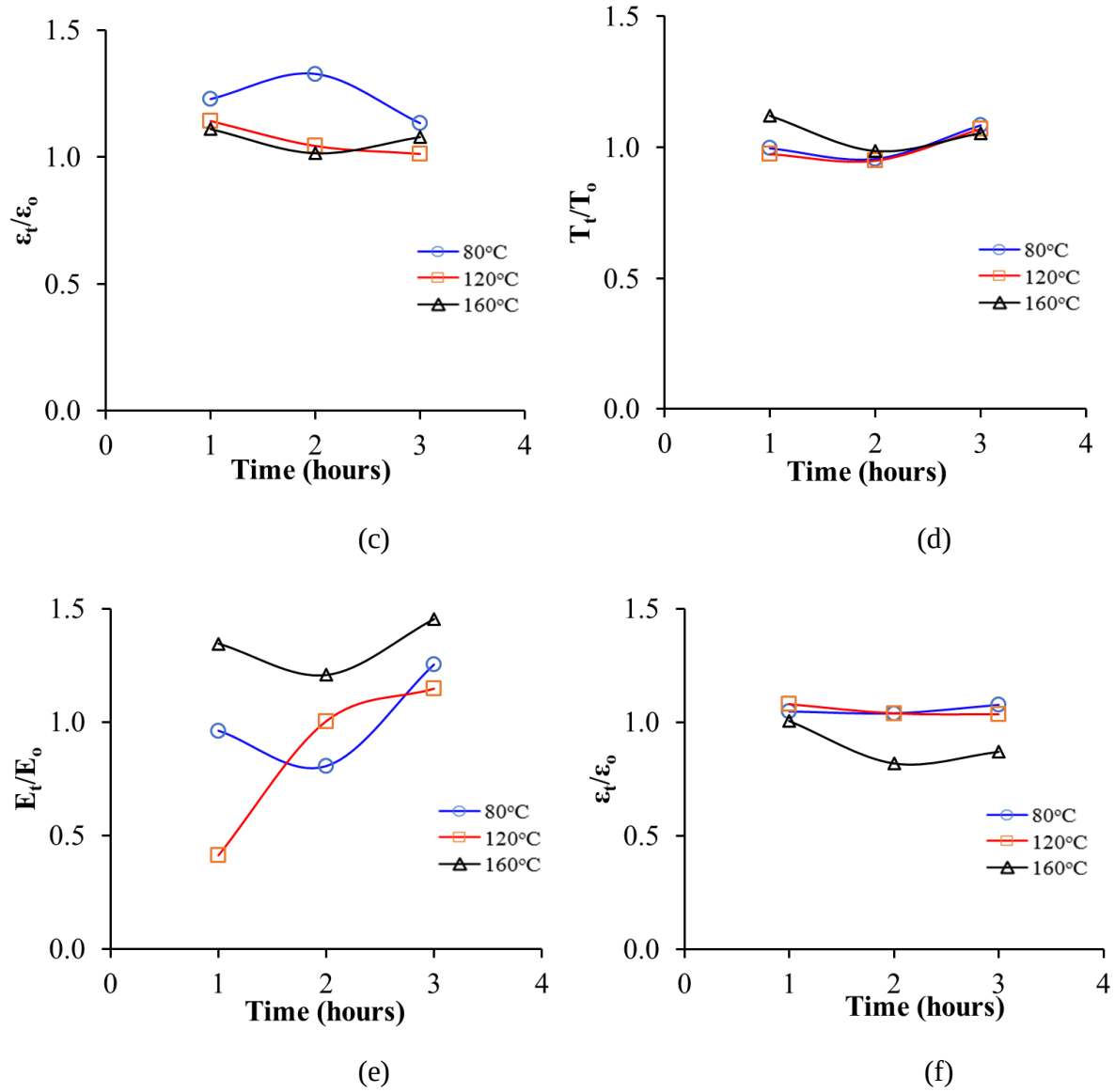

Fig. 3.11. Normalized curves of tensile characteristics of GFRP: (a) Tensile strength of specimen in 0^o fiber direction, (b) Youngs modulus of elasticity of specimen in 0^o fiber direction, (c) Failure strain of specimen in 0^o fiber direction, (d) Tensile strength of specimen in 90^o fiber direction, (e) Youngs modulus of elasticity of specimen in 90^o fiber direction, (f) Failure strain of specimen in 90^o fiber direction.

In 0^o fibers aligned GFRP specimens, elastic and inelastic energies of specimens with respect to curing time and temperature is shown in Fig. 3.12(c). GFRP specimen (T0-G80-2) cured at 80^{o}C temperature for two hours has high inelastic energy which is due to high failure strain. It is noticed that variation of total energy absorbed by specimen for different curing temperature and time is

proportional to the failure strain of the specimens. It is worth mentioning that inelastic energy is higher than total energy of room temperature cured specimens. Like CFRP laminates, inelastic energy absorbed in 90^{o} fiber aligned specimens is less than 0^{o} fiber aligned specimens (see Fig. 3.12(d)). The maximum energy absorbed by the specimen and the peak elastic energy can be observed in the specimen cured at 80^{o}C temperature for 1-hour duration. In case of 120^{o}C temperature cured specimens (Fig. 3.12(d)), increase in elastic energy was observed with increase in the time of curing. Thus Fig. 3.12 shows that energy absorbed by GFRP specimens is higher than CFRP specimens because GFRP specimens have high failure strains in comparison with CFRP specimens.

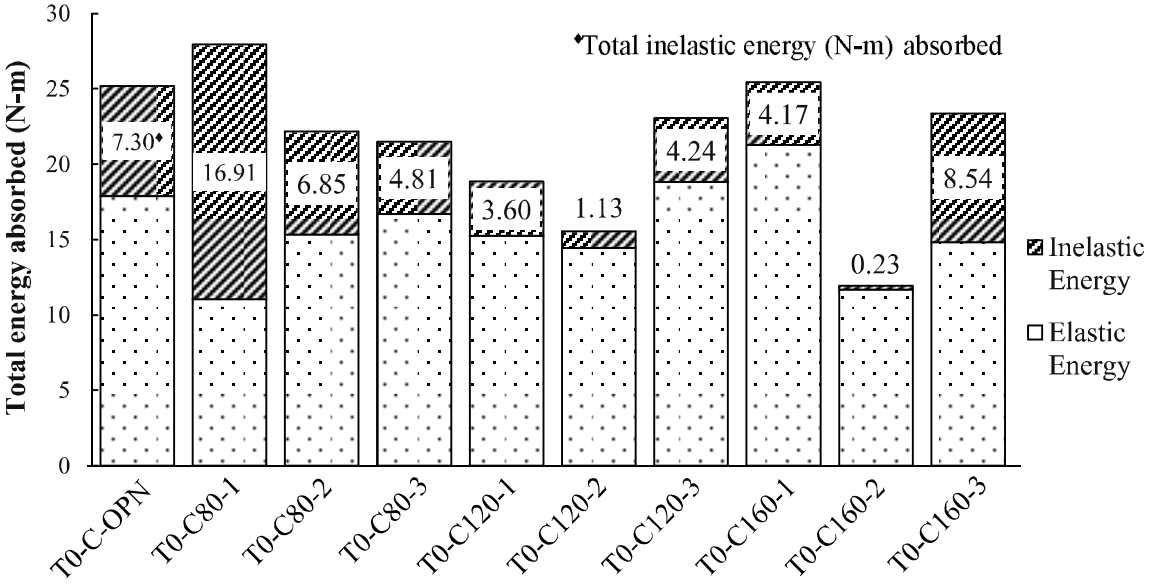

(a)

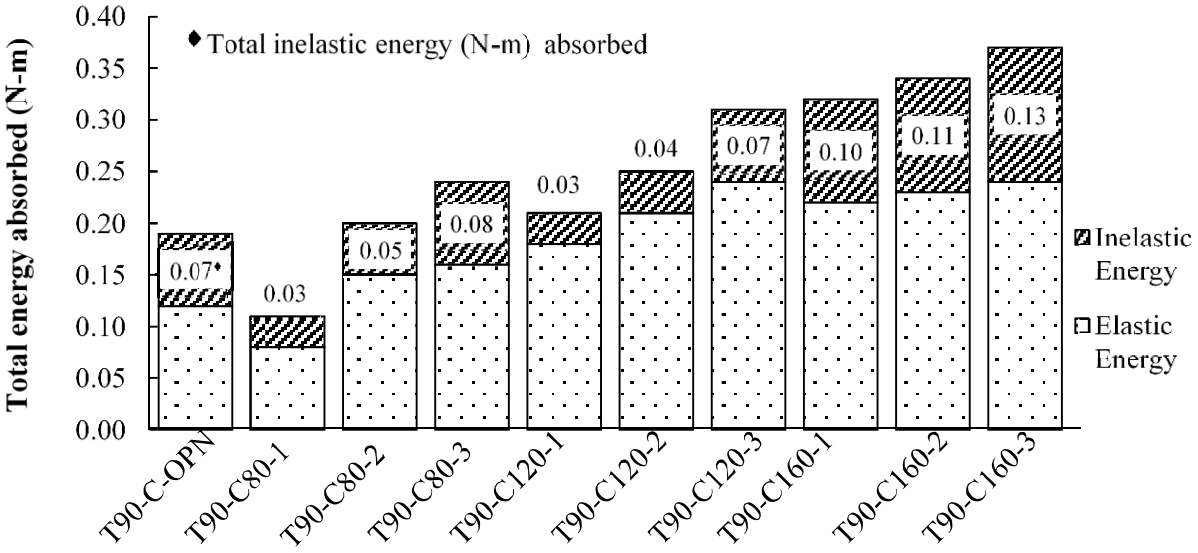
Total energy absorbed (N-m)
0.40
0.35
0.30
0.25
0.20
0.15
0.10
0.05
0.00
Total inelastic energy (N-m) absorbed
0.07
0.03
0.05
0.08
0.03
0.04
0.07
0.10
0.11
0.13
Inelastic Energy
Elastic Energy
T90-C-OPN
T90-C80-1
T90-C80-2
T90-C80-3
T90-C120-1
T90-C120-2
T90-C120-3
T90-C160-1
T90-C160-2
T90-C160-3

(b)

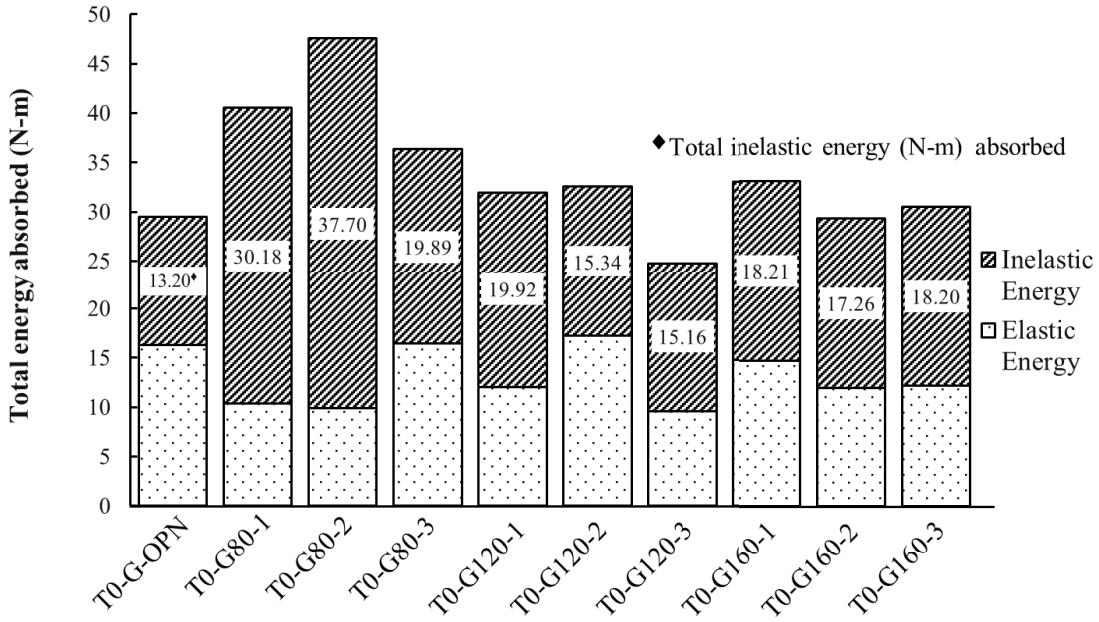
Total energy absorbed (N-m)
50
45
40
35
30
25
20
15
10
5
0
Total inelastic energy (N-m) absorbed
13.20
30.18
37.70
19.89
19.92
15.34
15.16
18.21
17.26
18.20
Inelastic Energy
Elastic Energy
T0-G-OPN
T0-G80-1
T0-G80-2
T0-G80-3
T0-G120-1
T0-G120-2
T0-G120-3
T0-G160-1
T0-G160-2
T0-G160-3

©

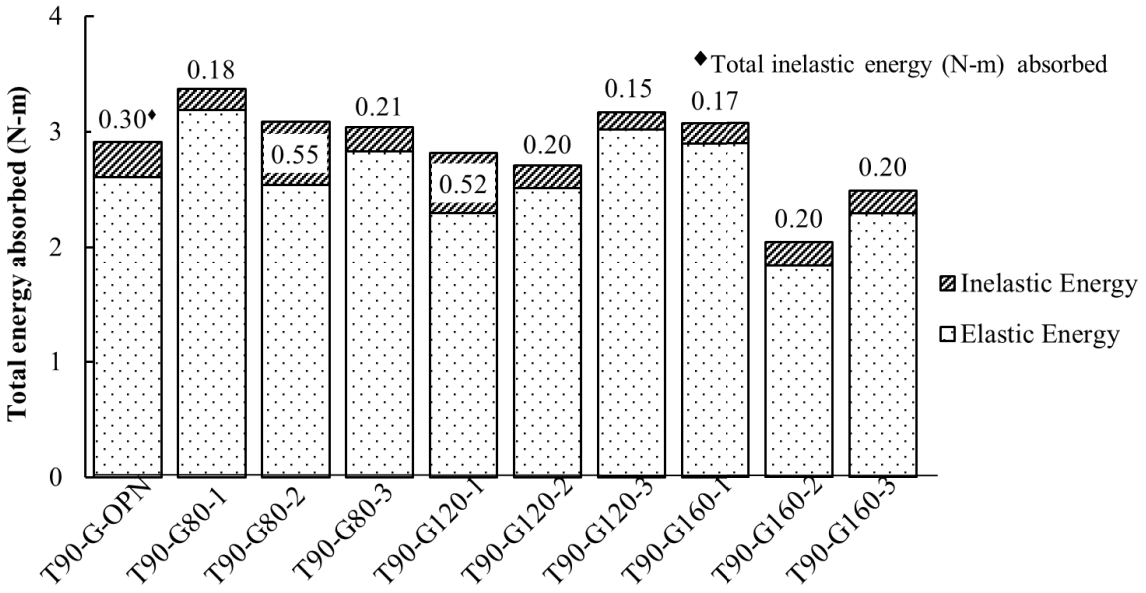

(d)

Fig. 3.12. Energy absorbed by FRP specimens: (a) 0^o fiber aligned CFRP, (b) 90^o fiber aligned CFRP, (c) 0^o fiber aligned GFRP, (d) 90^o fiber aligned GFRP

3.4.1.4. Shear Modulus

In this study, shear modulus of laminates is determined by testing of 45^o fiber aligned specimens and calculated from Eq. (3). As expected, all 45^o fiber aligned CFRP and GFRP specimens failed by aligned gage middle (AGM) failure in the gage length of the specimen along the direction of fiber as shown in Figs. 3.13(a) and 3.14(a). Variation of shear modulus of all hot air oven and room temperature cured CFRP and GFRP laminates is described in Figs. 3.13(b) and 3.14(b), respectively. CFRP specimens which are cured at elevated temperature have lower shear modulus (Fig. 3.13(b)) than that of open air cured specimens, while the GFRP specimens cured at temperature of 160^oC have higher shear modulus than that of open air cured specimens (see Fig. 3.14(b)) for all curing durations. It is stated that with increase in the temperature of curing of CFRP laminates, shear modulus decreases. Normalized curves of CFRP and GFRP specimens cured at elevated temperature and various durations having variation of shear modulus with respect to the room temperature is shown in Figs. 3.15(a) and 3.15(b), respectively.

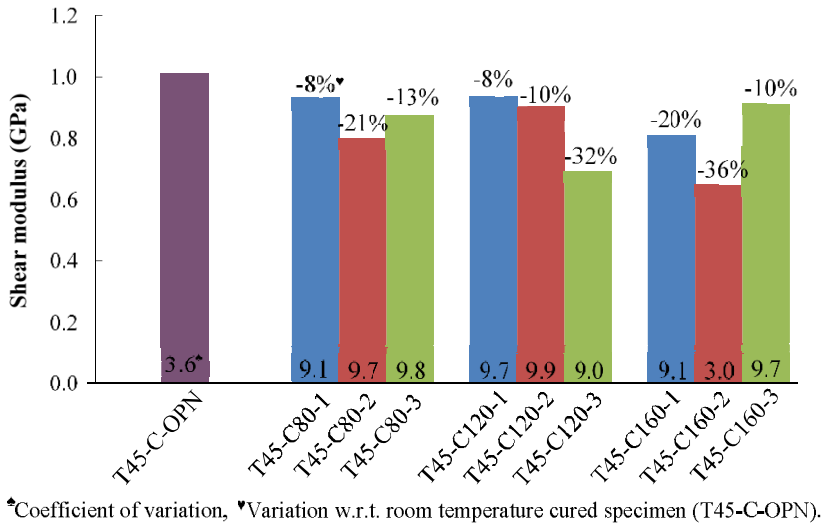

Fig. 3.13. Characteristics of 45^{o} fiber aligned CFRP specimens: (a) Failure mode, (b) Shear modulus

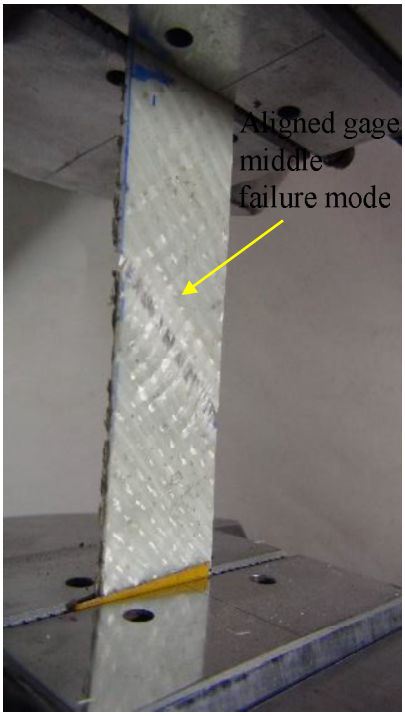

(a)

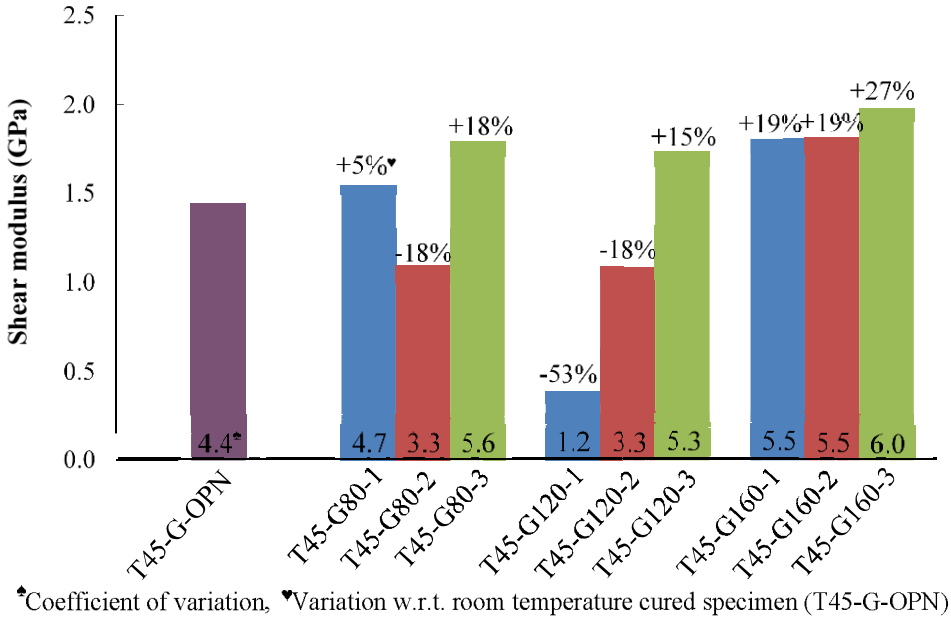

(b)

Fig. 3.14. Characteristics of 45° fiber aligned GFRP specimens: (a) Failure mode, (b) Shear modulus

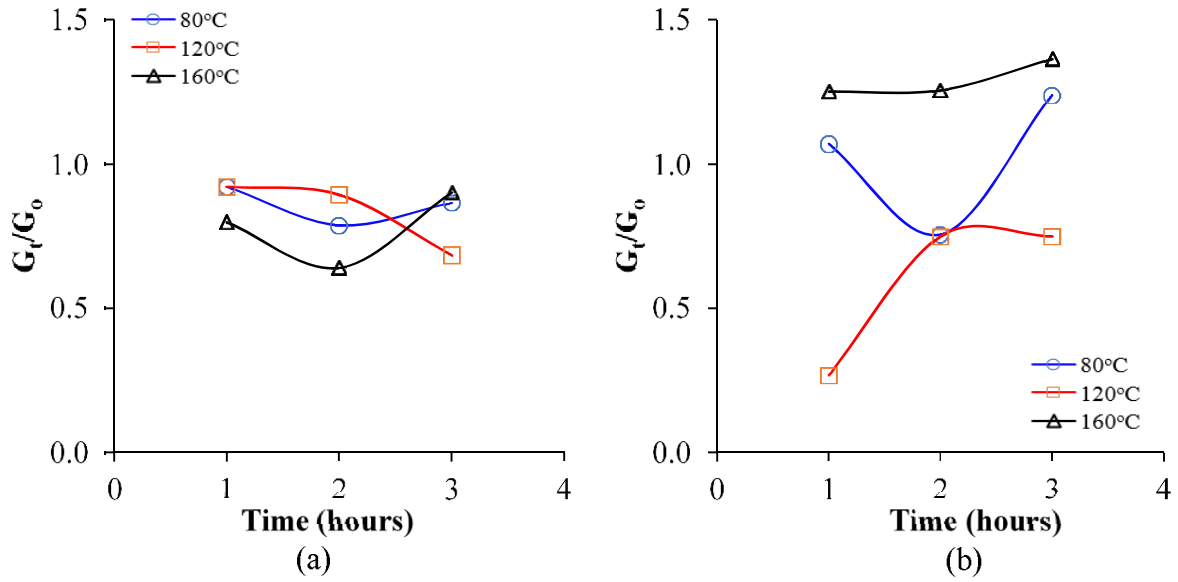

Fig. 3.15. Normalized curves of shear modulus of the specimens aligned 45° to the fiber direction: (a) CFRP, (b) GFRP

3.4.1.5. Failure modes

Failure modes of specimens under uniaxial tensile loading are shown in Fig. 3.16 while stress strain curves of the plain FRP and functionally graded hybrid specimens are shown in Figs. 3.17 and 3.18, respectively. CFRP specimens failed in very brittle manner as shown in Fig. 3.17(a) while the progressive failure of GFRP specimens was observed in Fig. 3.17(b) and the stress-strain curves of GFRP specimens also show the failure of fibers gradually. In SH specimens, where glass fibers are sandwiched in between carbon fibers, i.e., T-SH-(CCGG)s, transverse splitting of carbon fibers were observed in the middle of gauge length of the specimens, due to which delamination is produced in between glass and carbon fibers. Further, glass fibers failed, which led to the complete loss in the load carrying capacity of the specimens. Due to the failure of specimens in stepwise manner, progressive failure was observed in the stress-strain curves of T-SH-(CCGG)s specimens. In contrary, specimens having carbon fibers sandwiched in between the glass fibers (T-SH-(GGCC)s) has shown catastrophic failure. It is due to the first failure of carbon fibers which are the middle layers of the laminate, led to the complete loss of load carrying capacity of the specimen. During testing of T-SH-(GGCC)s specimens, on the failure of CFRP layers, gunshot sound occurred and the stress-strain curves of these specimens also show complete loss in load

carrying capacity just after the peak load as shown in Fig. 3.17(d). Similar behavior was seen in specimen T-AH-(CGCG)s as shown in Fig. 3.17(e). Specimens having alternate layers of glass and carbon fibers T-(AH-(GCGC)s) show bilinear stress-strain curve [Fig. 3.17(f)], that means internal fibers in the specimen failed, because, during testing no cracks were seen on the specimens and minute cracking sound was heard at that particular stress where curve changes its slope.

Comparison of functionally graded hybrid (FH) specimens with other hybrid specimens have shown nonlinear response before ultimate load as shown in Fig. 3.18, which is due to the functional gradation of carbon fibers with glass fibers. During the tensile testing of FH specimens having carbon fibers functionally graded around glass fibers [T-FH-(CG)s-I, T-FH-(CG)s-II and T-FH-(CG)s-III], carbon fibers at the surface were split out like sharp spikes. The combined splitting of fibers and longitudinal cracking was observed in one type of the functionally graded hybrid specimens T-FH-(CG)s-II. Due to the splitting of fibers, cracks propagated along the gauge length of the specimens under tensile loading. Though these specimens have ductile nature, fracture occurred in a detonating manner just after peak load [Fig.s 3.18(a), 3.18(b) and 3.18(c)], due to the failure of proportioned carbon fibers in the specimen.

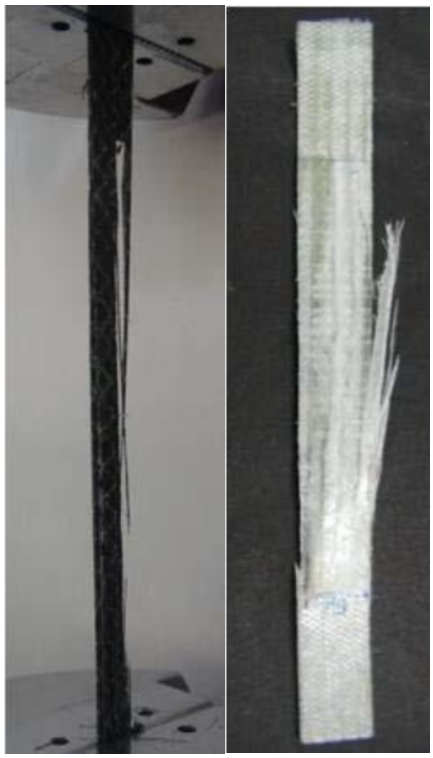

(a) (b)

Fig. 3.16. Failure modes of specimens under tension, (a) T-(CCCC)s (b) T-(GGGG)s

On the other hand, FH specimens in which glass fibers are functionally graded around with carbon fibers [T-FH-(GC)s-I, T-FH-(GC)s-II, and T-FH-(GC)s-III], under tensile loading, cracking sounds were heard gradually and the corresponding cracks in the thickness direction appeared in the gauge length of the specimen. As a result, delamination between carbon and glass fibers was produced. In comparison of these FH specimens [T-FH-(GC)s-I, T-FH-(GC)s-II and T-FH-(GC)s-III] as shown in Fig.s 3.18(d), 3.18(e) and 3.18(f) with SH specimen [T-SH-(GGCC)s], it is concluded that functional gradation of glass fibers around carbon fibers produces progressive failure.

3.4.1.6. Strength, stiffness and failure strain

The mechanical properties of the hybrid specimens with respect to the plain CFRP and glass fiber reinforced polymer (GFRP) laminated specimens is presented in Table 3.6. Among all hybrid composites, the maximum tensile strength is observed in functionally graded hybrid specimen T-FH-$(CG)_s$-II, in which carbon fibers are linearly graded around glass fibers, i.e., glass fibers are in core, and specimen T-FH-$(CG)_s$-I shows the highest modulus.

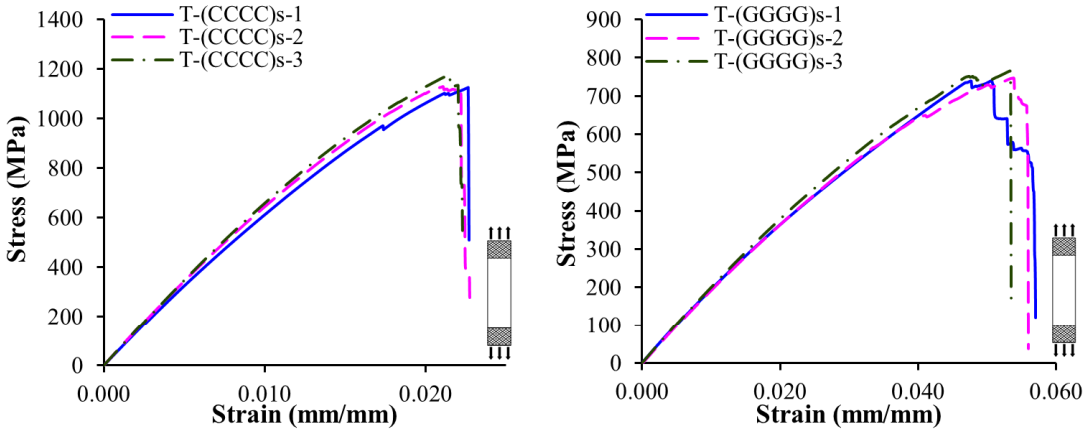

(a) (b)

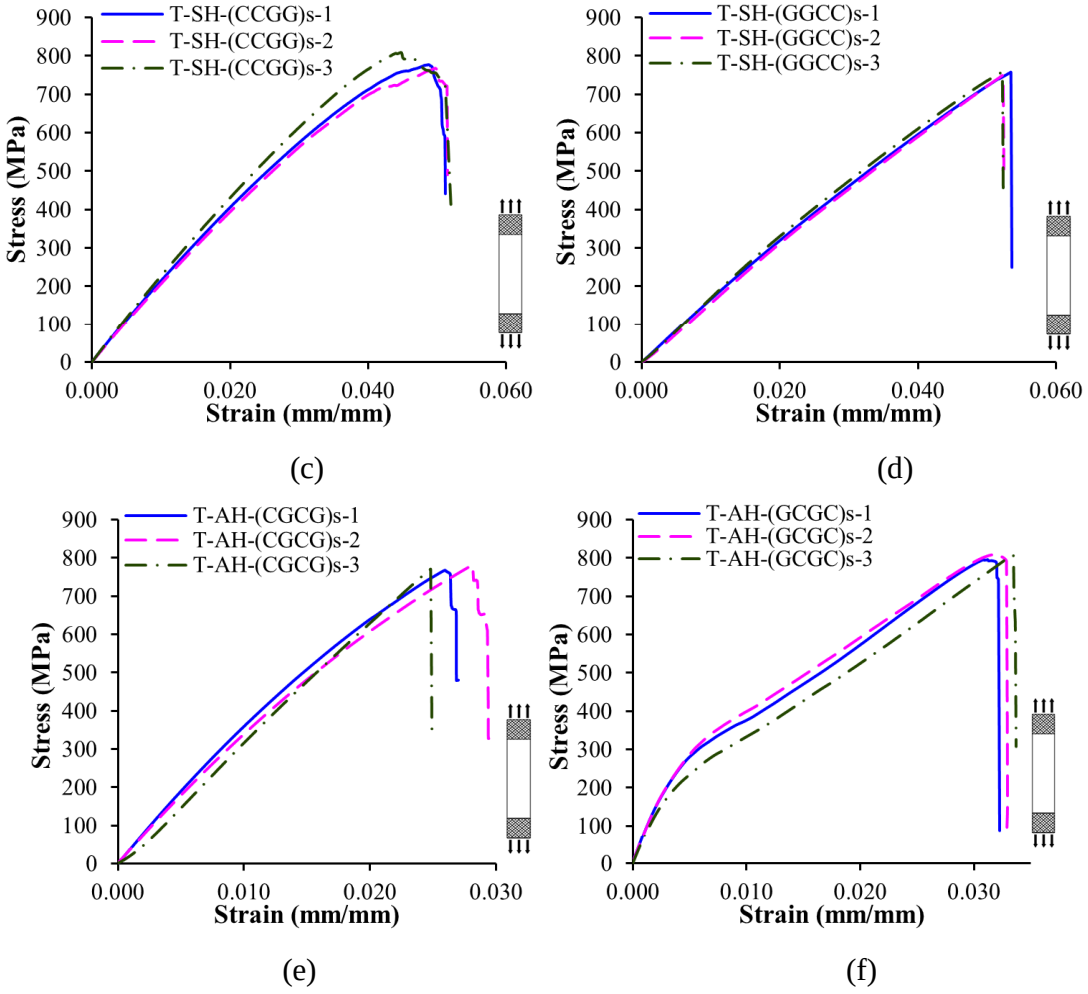

Fig. 3.17. Stress-strain graphs of plain FRP, sandwich hybrid (SH), and alternate hybrid (AH) tensile specimens: **(a)** T-$(CCCC)_s$; **(b)** T-$(GGGG)_s$; **(c)** T-SH-$(CCGG)_s$; **(d)** T-SH-$(GGCC)_s$; **(e)** T-AH-$(CGCG)_s$; **(f)** T-AH-$(GCGC)_s$

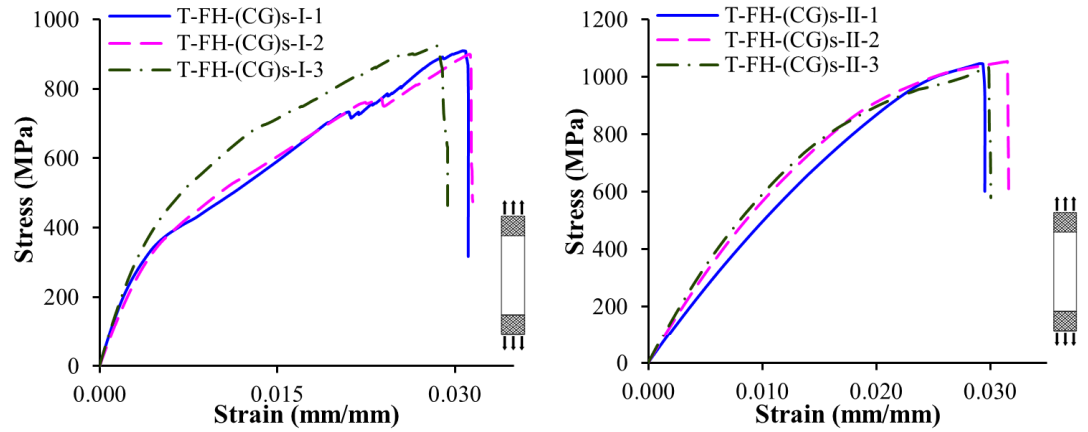

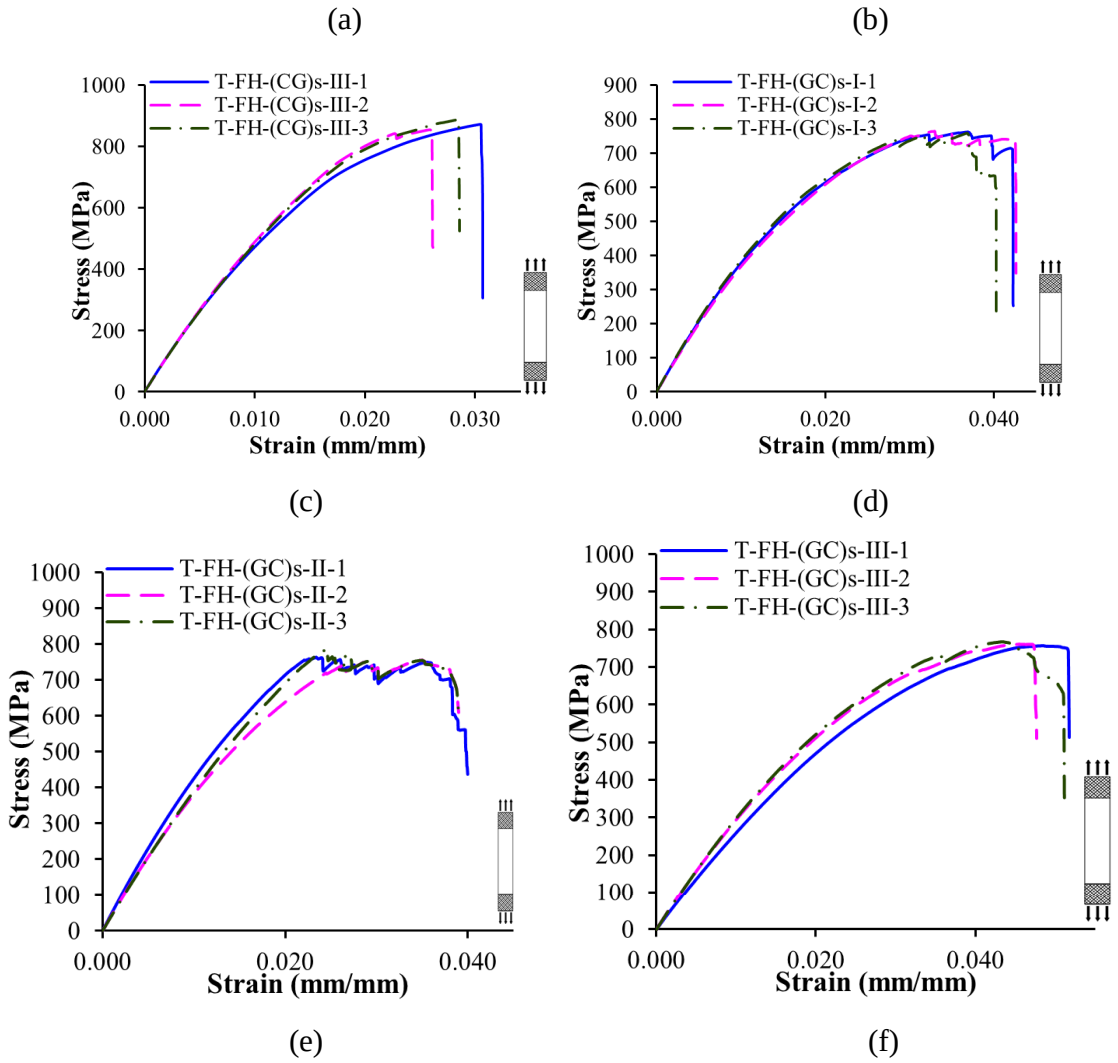

Fig. 3.18. Stress-strain graphs of tensile functionally graded hybrid (FH) specimens: **(a)** T-FH-$(CG)_s$-I; **(b)** T-FH-$(CG)_s$-II; **(c)** T-FH-$(CG)_s$-III; **(d)** T-FH-$(GC)_s$-I; **(e)** T-FH-$(GC)_s$-II; **(f)** T-FH-$(GC)_s$-III

It is noted that the functionally graded hybrid specimen having highest elastic modulus also offers second highest tensile strength than other sandwich and functionally graded hybrid specimens, and most importantly higher modulus than CFRP specimens. In other words, T-FH-(CG)s-I specimen shows positive hybrid effect with respect to CFRP in terms of elastic modulus. Further it is noticed that, functionally graded hybrid specimen T-FH-(CG)s-II (i.e., specimen which has glass fiber in its core and carbon as surface) has attained maximum tensile strength with respect to all hybrid specimens with 22% lower value than that of T-(CCCC)s specimen but it is higher than the GFRP specimens T-(GGGG)s.

Table 3.6. Mechanical properties of the specimens such as tensile strength, Young's modulus, failure strain, and energy absorbed

Specimen ID	Tensile strength (MPa)	Young's modulus (GPa)	Failure strain (mm/mm)	Elastic energy (N-m)	Inelastic energy (N-m)
T-CCCC	1145	62	0.023	8.11	6.82
T-GGGG	751	17	0.056	11.51	13.41
T-SH-CCGG	785	20	0.052	10.01	14.45
T-SH-GGCC	755	17	0.053	16.47	4.69
T-AH-CGCG	774	33	0.027	8.07	3.48
T-AH-GCGC	804	50	0.033	1.25	14.77
T-FH-$(CG)_s$-I	911	63	0.031	1.44	17.07
T-FH-$(CG)_s$ -II	1045	54	0.030	3.64	7.75
T-FH-$(CG)_s$ - III	871	48	0.028	4.38	4.85
T-FH-$(GC)_s$ -I	762	36	0.042	4.03	8.05
T-FH-$(GC)_s$ -II	769	36	0.038	4.92	15.24
T-FH-$(GC)_s$ - III	761	27	0.050	3.20	22.64

This indicates the existence of positive hybrid effect with respect to GFRP specimens. Percentage values in bar charts of figures (3.5, 3.6, 3.8, 3.9, 3.12, 3.13) indicate hybrid effect with respect to CFRP or GFRP as given at bottom of each bar chart. Functionally graded hybrid specimens in which glass fibers are in the core and carbon fibers are at exterior offers higher strength and stiffness but lower failure strain and vice-versa. Along with, specimens with glass fiber in the core region has highest tensile strength and stiffness than its vice-versa. It is worth to mention that functional gradation of carbon fibers around glass fibers proves to be better than SH laminates in terms of providing strength and stiffness simultaneously. Moreover, in case of failure strain parameter, the specimens with carbon fiber in the middle layer have maximum failure strain as shown in Table 3.6 compared to the specimens with glass fiber in the core.

From theoretical analysis, the laminate T-AH-(CGCG)s initially fails at an average tensile stress of 773 MPa which is a near value to tensile stress obtained from experimental investigation.

Similar analysis is followed in case of tensile strength of the specimen T-FH-(CG)s-I and the laminate failed at a tensile stress of 924 MPa which is a closer value to the obtained experimental tensile stress, i.e., 911 MPa of the same specimen. This signifies that theoretical values are in good agreement with the experimental values.

Elastic and inelastic energy absorbed by hybrid and non-hybrid specimens are shown in Fig. 3.19. Sandwich hybrid specimen T-SH-(GGCC)s absorbed highest elastic energy amongst all specimens including plain CFRP and GFRP specimens (see Fig. 3.19) while the highest inelastic energy was absorbed by functionally graded specimen with layup configuration T-FH-(GC)s-III among all composites. Even though total energy absorbed by T-(GGGG)s, T-SH-(CCGG)s and T-FH-(GC)s-III specimens is same, but the inelastic energy absorbed by the T-FH-(GC)s-III specimen is very high, therefore this specimen is more ductile in nature.

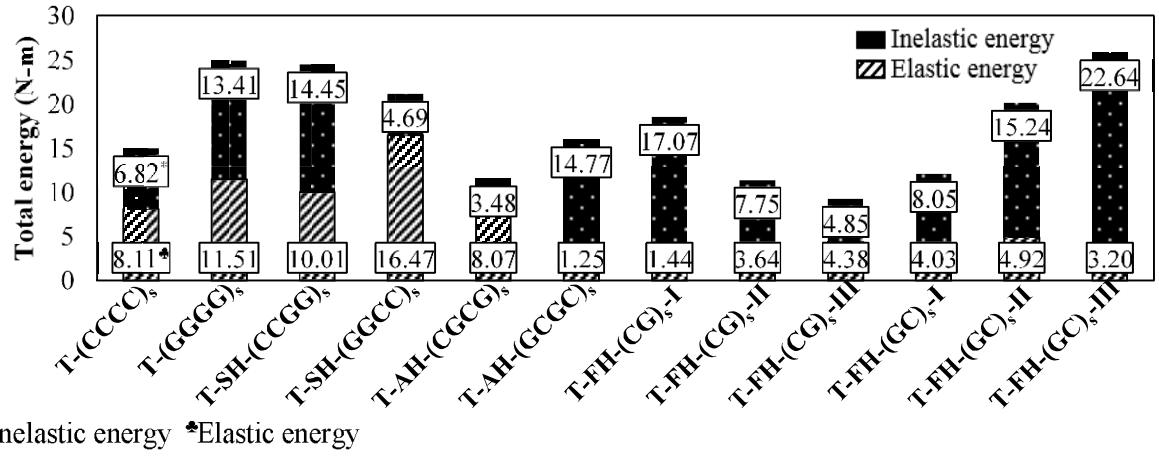

Fig. 3.19. Total energy absorbed by the plain, sandwich hybrid, alternate hybrid and functionally graded hybrid specimens

3.4.2. Compressive characteristics

3.4.2.1. CFRP laminates

The mode of failure of CFRP specimens under compression is brooming gage middle (BGM) failure which means broomed fractures as shown in Fig. 3.20(a). The average compressive strength of each laminate is shown through bar chart of Fig. 3.20(b). The maximum compressive strength of 0^o fiber aligned CFRP specimens is observed in C0-C80-3 specimen, which is 3% greater than the CFRP specimens cured at room temperature (see Fig. 3.20(b)). It is noticed that compressive strength of specimens increases with increase in curing duration at 90^oC. However, this trend is

absent in 160^{o}C temperature cured specimens with a minor difference among their strength parameters. Moreover, the failure strain (Fig. 3.20(c)) in the room temperature cured specimens is high with only 3% deviation than C0-C160-3 specimen which has dominant failure strain among temperature cured specimens (see Fig. 3.20(c)). It is also worth mentioning that specimens cured for three hours have higher failure strain than that of 1 and 2 hour cured specimens.

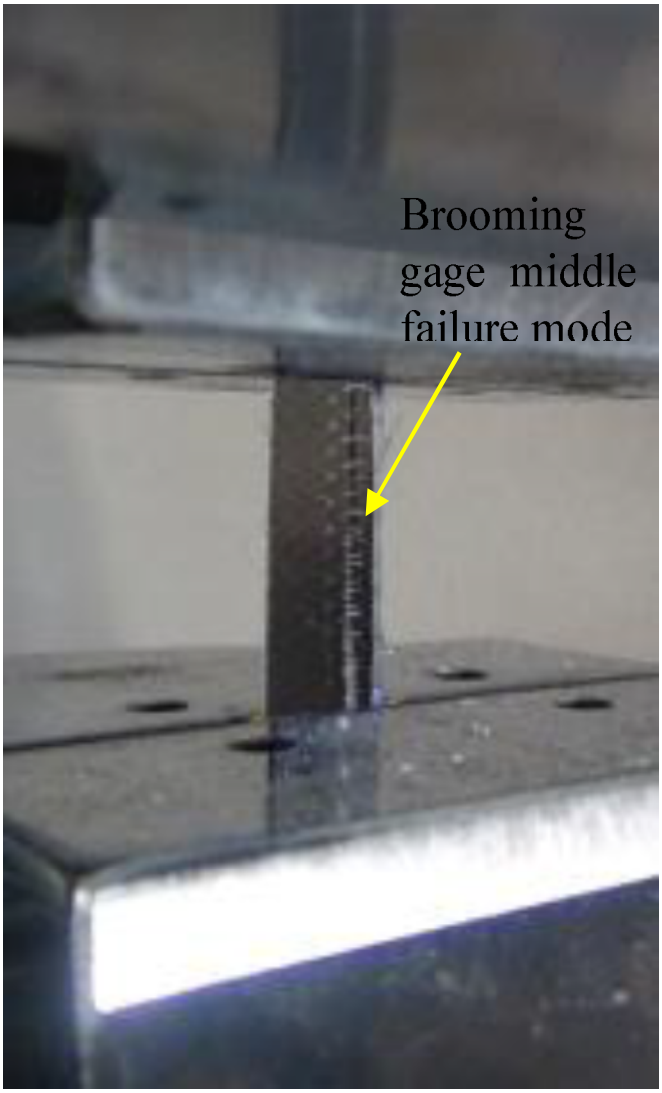

(a

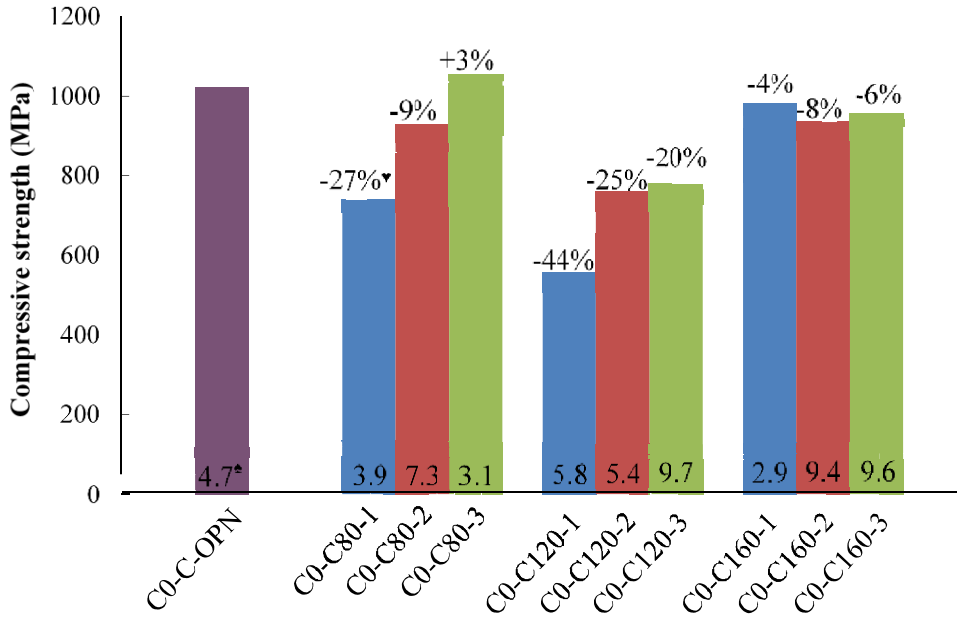

♠Coefficient of variation, ♥Variation w.r.t. room temperature cured specimen (C0-C-OPN).

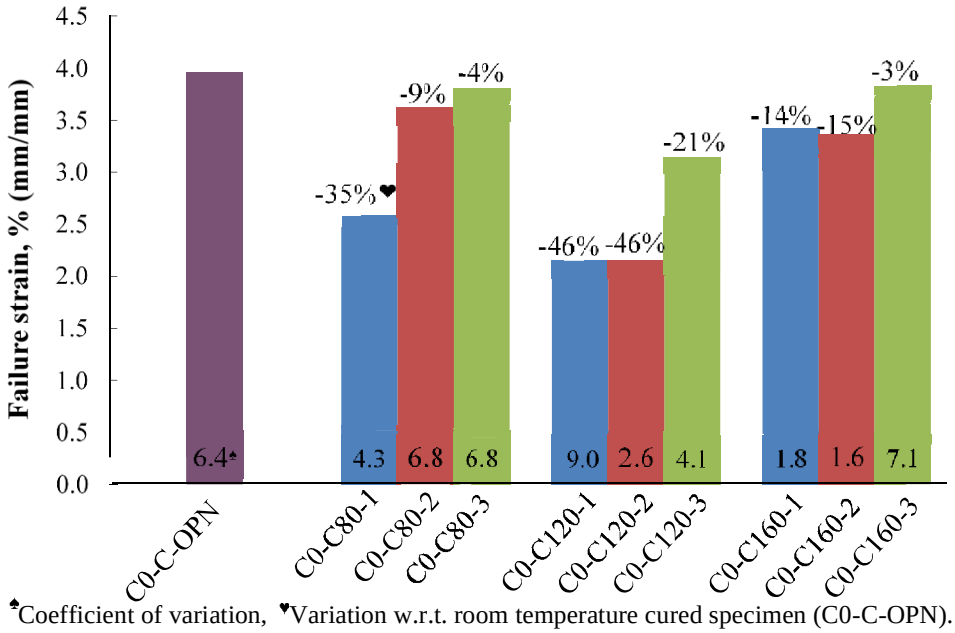

♠Coefficient of variation, ♥Variation w.r.t. room temperature cured specimen (C0-C-OPN).

(c)

Fig. 3.20. Compressive test results of 0^{o} fiber aligned CFRP specimens: (a) Failure mode, (b) Compressive strength, (c) Failure strain.

In CFRP specimens having fiber orientation 90^{o} failed by through thickness gage middle (HGM) failure (see Fig. 3.21(a)). Compressive strengths of the specimens having fiber aligned normal to the loading direction are presented in a bar chart format as presented in Fig. 3.21(b). It is observed that laminates C90-C160-2 and C90-C80-2 have highest transverse compressive strength which is 19% and 18% higher than that of room temperature cured specimens, respectively. It is also noticed that specimens cured for two hours at a temperature have higher transverse compressive strength than that of 1-hour and 3-hour duration curing. The failure strain of the specimens cured at room temperature is lower than temperature cured specimens (see Fig. 3.21(c)). Failure strain was observed to increase with time for 120^{o}C and 160^{o}C temperature cured specimens which have better failure strains comparatively. Curing of laminates at temperature of 120^{o}C and 160^{o}C for three hours have shown significantly high failure strain with respect to the open-air cured laminates, i.e., 44% and 51% higher values, respectively. Figs 3.22(a) and 3.22(b), respectively show the normalized compressive strength and failure strains for CFRP specimens with 0^{o} fiber alignment. Corresponding curves of 90^{o} fiber aligned specimens are illustrated in Figs. 3.22(c) and 3.22(d) constituting compressive strength and failure strain.

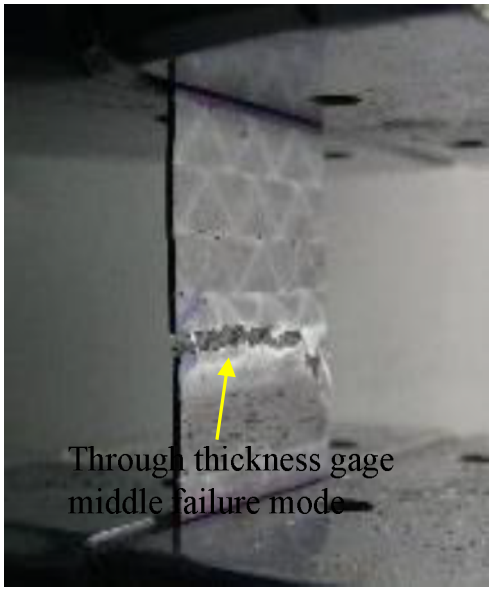

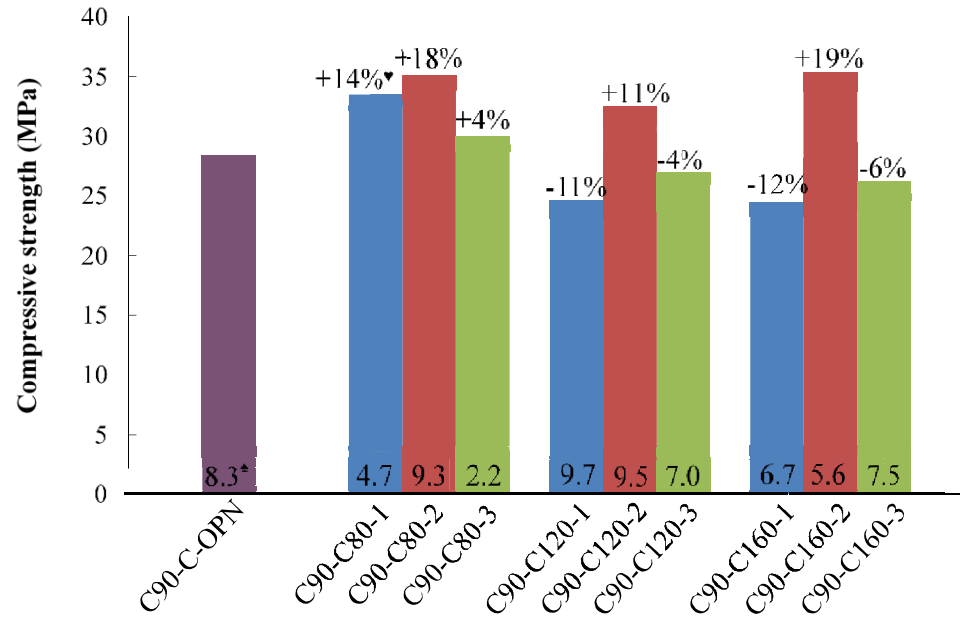

♠Coefficient of variation, ♥Variation w.r.t. room temperature cured specimen (C90-C-OPN).

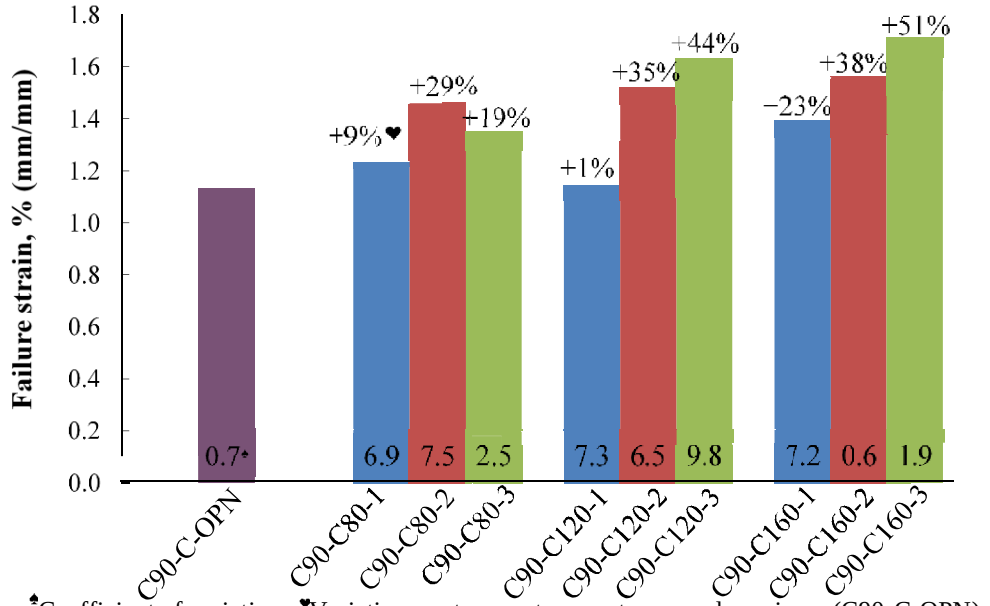

♠Coefficient of variation, ♥Variation w.r.t. room temperature cured specimen (C90-C-OPN).

(c)

Fig. 3.21. Compressive test results of 90º fiber aligned CFRP specimens: (a) Failure mode, (b) Compressive strength, (c) Failure strain.

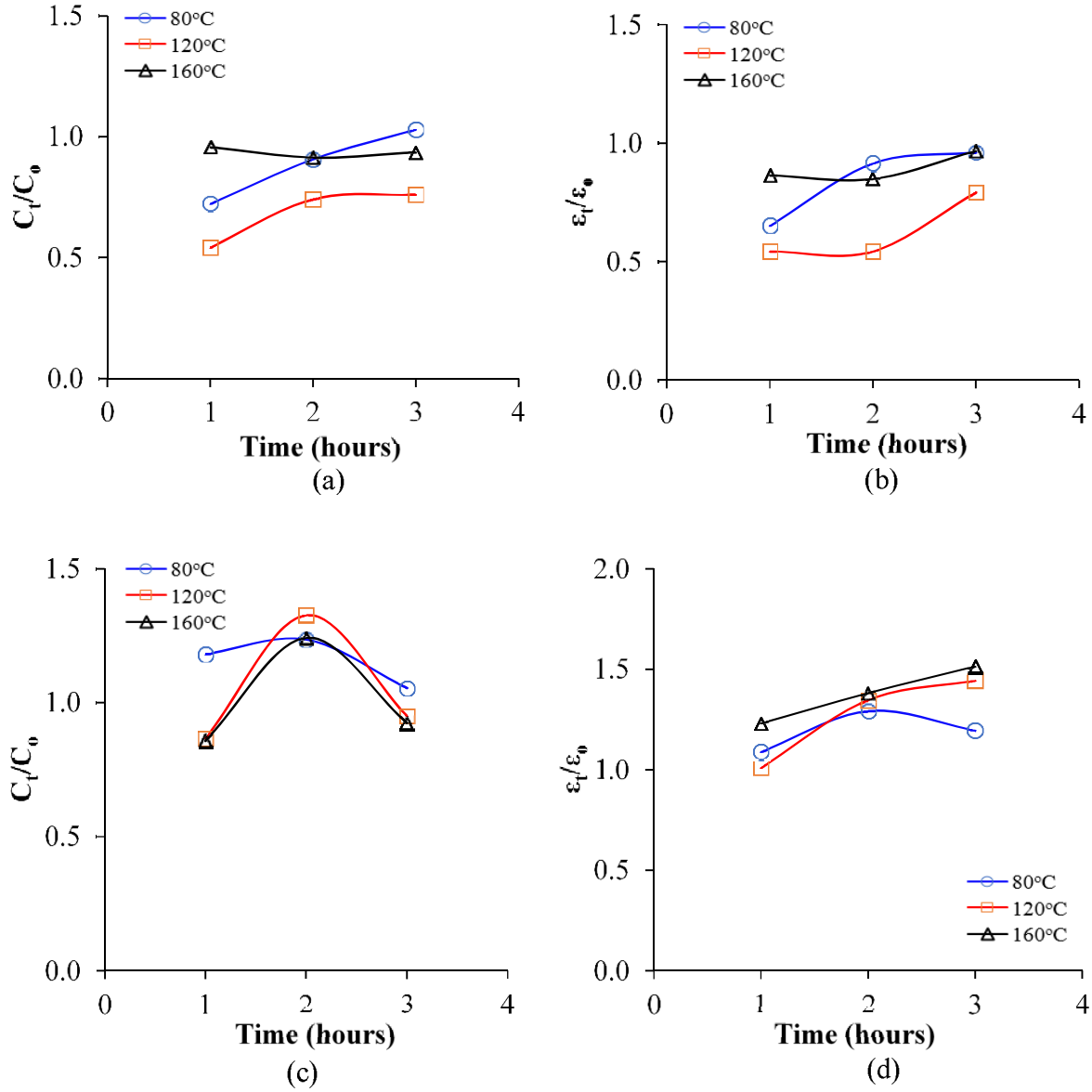

Fig. 3.22. Normalized curves of compressive characteristics of CFRP specimens: (a) Compressive strength of 0º fiber aligned specimens, (b) Failure strain of 0º fiber aligned specimens, (c) Compressive strength of 90º fiber aligned specimens, (d) Failure strain of 90º fiber aligned specimens.

3.4.2.2. GFRP laminates

Compressive tests of GFRP specimens having fiber orientation 0^o have shown the brooming gage middle (BGM) failure as depicted in Fig. 3.23(a). The average compressive strength and failure strain of GFRP specimens are shown in Figs. 3.23(b) and 3.23(c), respectively. It is observed that compressive strength and failure strain of oven cured GFRP laminates are comparatively higher than that of laminates cured at room temperature. It is worth mentioning that specimens C0-G80-1 has higher compressive strength and failure strain than room temperature and other oven cured specimens and the same trend is observed for failure strain of GFRP laminates. This specimen has 11% and 29% higher compressive strength and failure strain than room temperature cured specimens, respectively (see Fig. 3.23(b & c)).

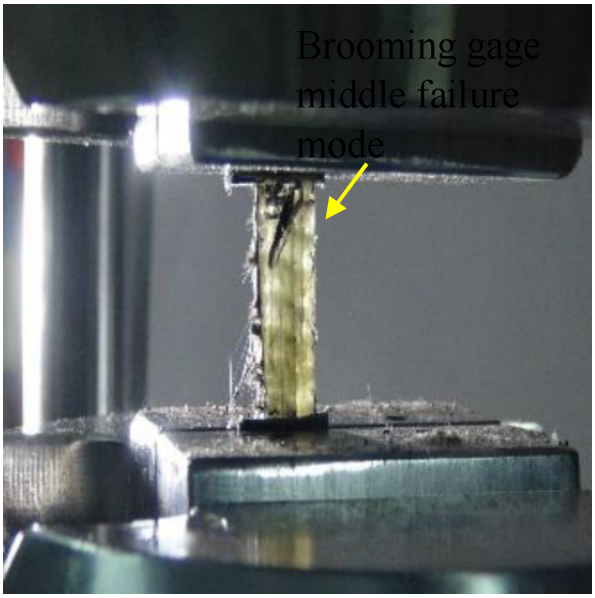

(a)

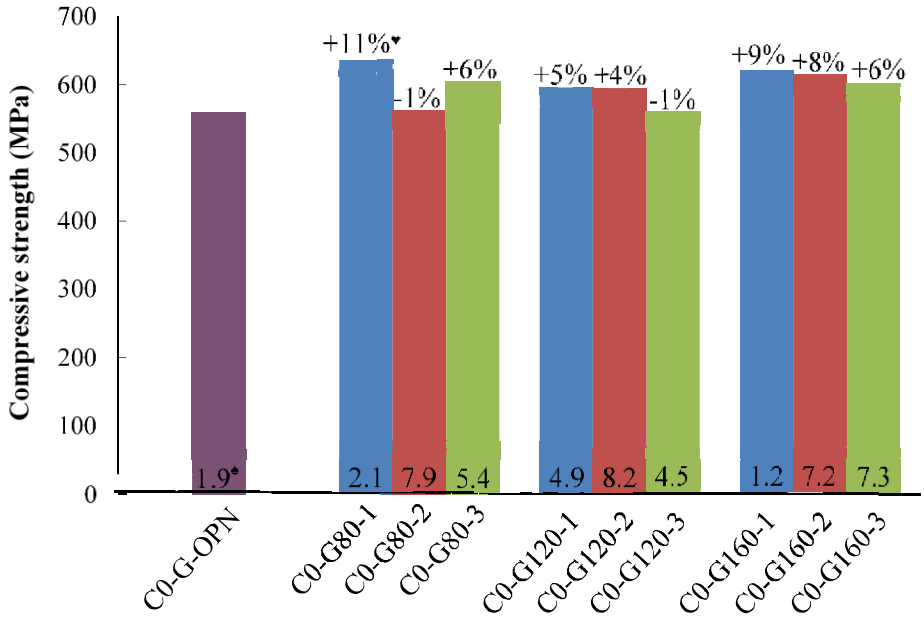

♠Coefficient of variation, ♥Variation w.r.t. room temperature cured specimen (C0-G-OPN).

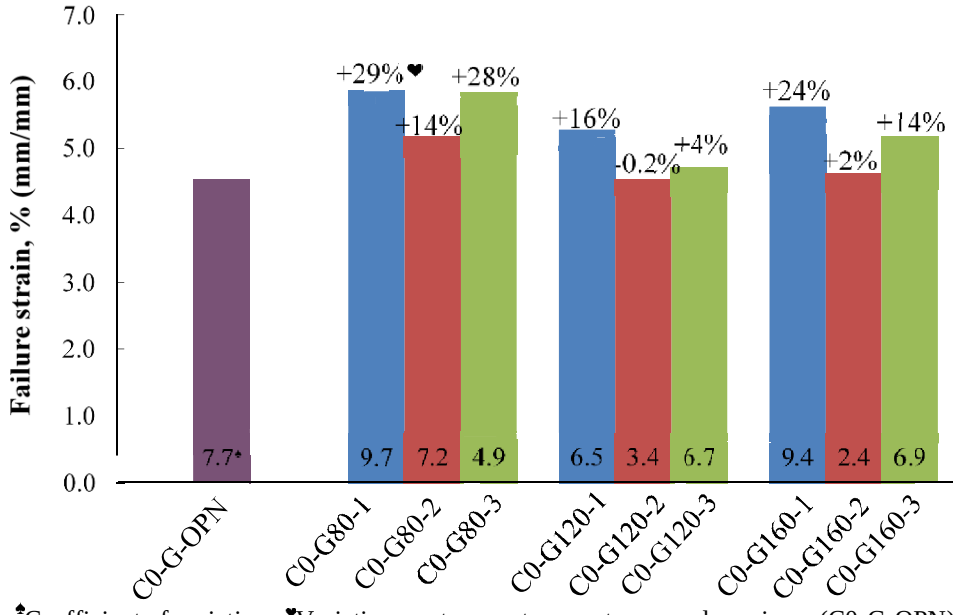

♠Coefficient of variation, ♥Variation w.r.t. room temperature cured specimen (C0-G-OPN).

(c)

Fig. 3.23. Compressive test results of 0^{o} fiber aligned GFRP specimens: (a) Failure mode, (b) Compressive strength, (c) Failure strain.

Through thickness gage middle (HGM) failure type was observed (see Fig. 3.24(a)) in compression testing of 90^{o} fiber aligned GFRP specimens. Like longitudinal compressive strength of GFRP laminates, maximum transverse strength is higher in laminates cured at temperature of 80^{o}C for 1-hour and the strength of this laminate is 12% higher than the specimens cured at room temperature (see Fig. 3.24(b)). Transverse compressive failure strain of room temperature cured specimens is lower than temperature cured specimens (see Fig. 3.24(c)), with a maximum difference of 48%. The ratio of compressive characteristics of oven cured specimens to the room temperature cured specimens in terms of compressive strength and failure strain of 0^{o} GFRP specimens is shown in Figs. 3.25(a) and 3.25(b) respectively, while for 90^{o} fiber aligned GFRP specimens, these normalized curves are shown in Figs. 3.25(c) and 3.25(d) respectively.

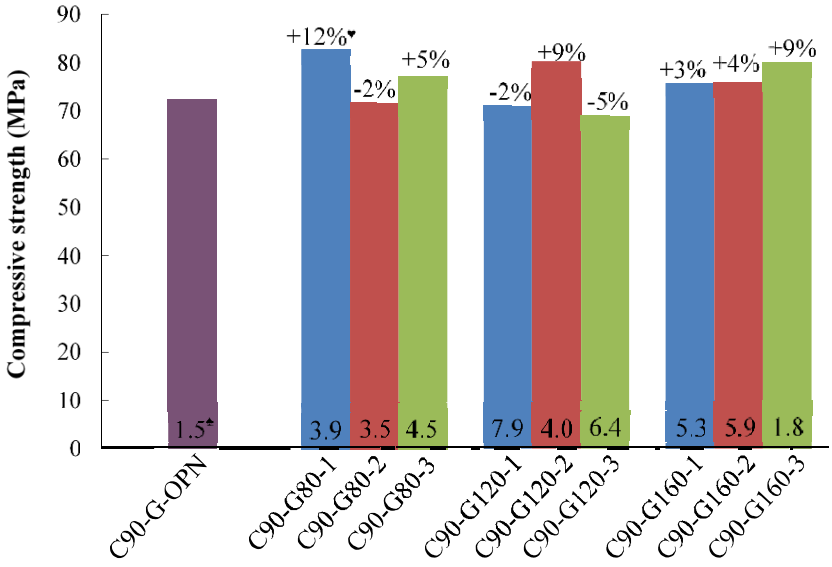

♠Coefficient of variation, ♥Variation w.r.t. room temperature cured specimen (C90-G-OPN).

(b)

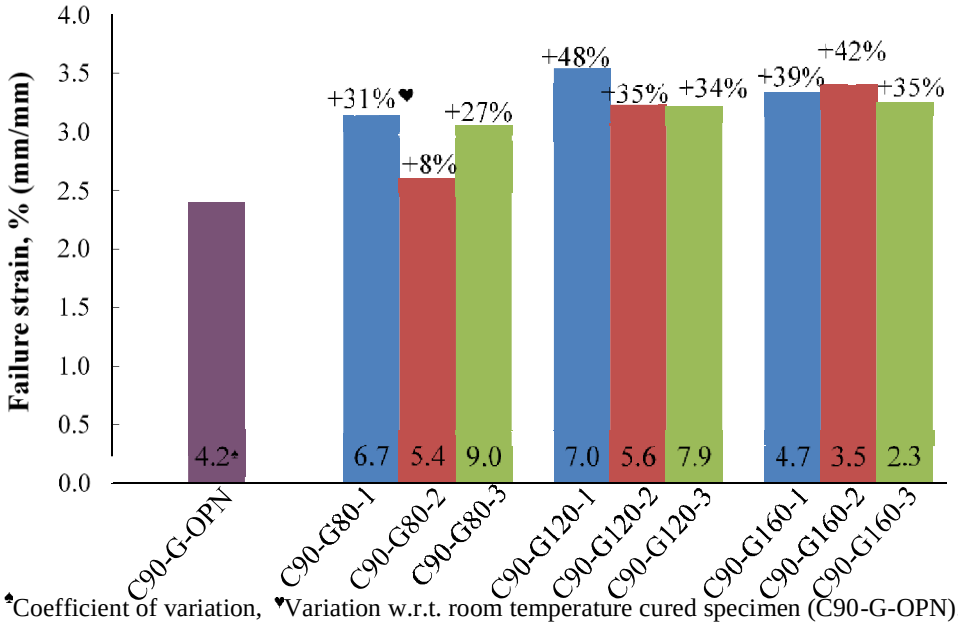

♠Coefficient of variation, ♥Variation w.r.t. room temperature cured specimen (C90-G-OPN).

(c)

Fig. 3.24. Compressive test results of 90° fiber aligned GFRP specimens: (a) Failure mode, (b) Compressive strength, (c) Failure strain.

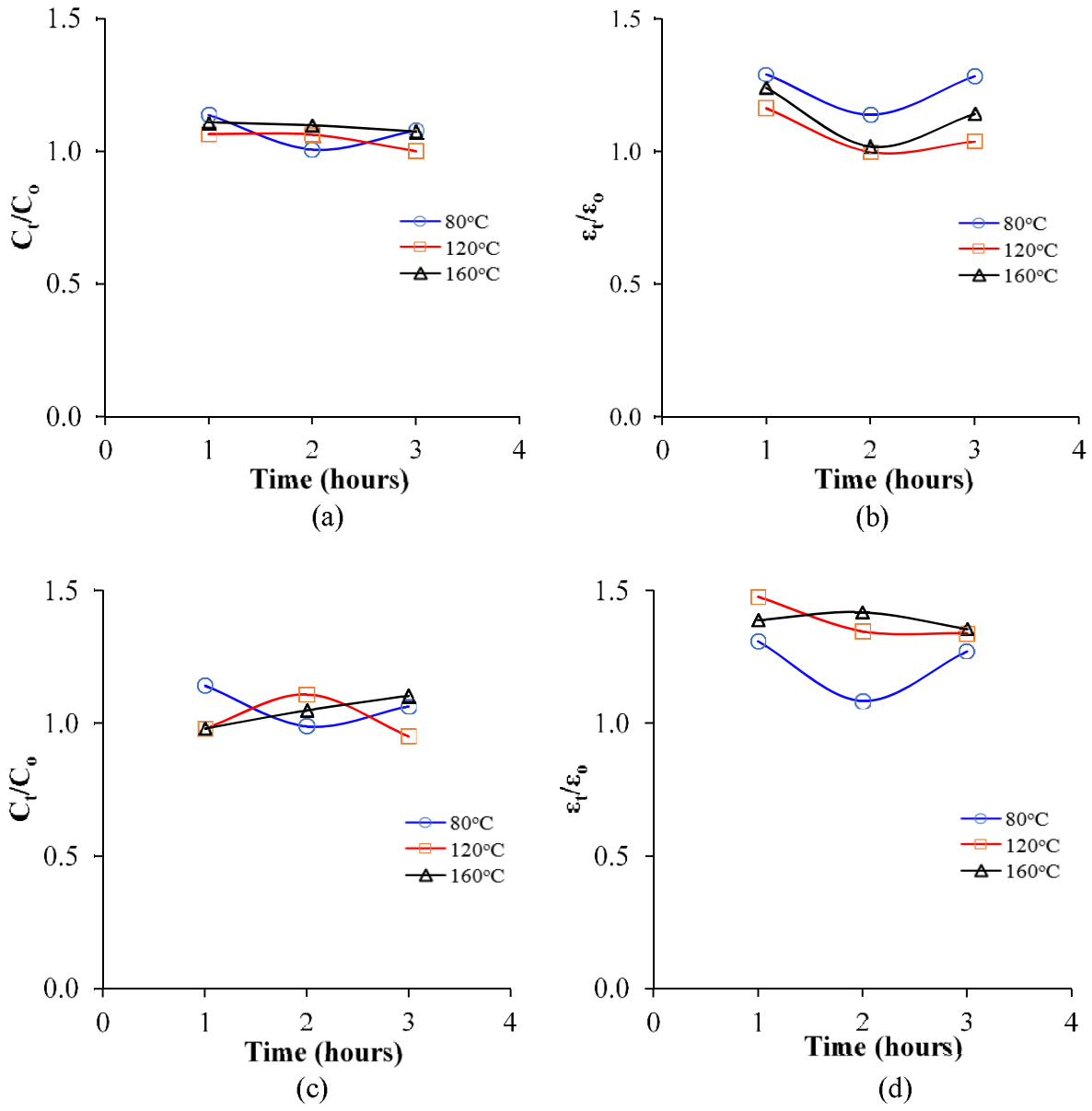

Fig. 3.25. Normalized curves of compressive characteristics of GFRP specimens: (a) Compressive strength of 0° fiber aligned specimens, (b) Failure strain of 0° fiber aligned specimens, (c) Compressive strength of 90° fiber aligned specimens, (d) Failure strain of 90° fiber aligned specimens.

3.4.2.3. Failure modes

Failure mode of non-hybrid compressive composites is shown in Fig. 3.26, and the stress-strain curves of non-hybrid, sandwich and alternate layers hybrid specimens obtained from compression testing are shown in Fig. 3.27. Under uniaxial compressive load, the SH, alternate layers hybrid and functionally graded hybrid specimens underwent failure such as crushing of fibers, delamination of fibers, kink fractures (see Fig. 3.26), and combined crushing and buckling. CFRP specimens failed by transverse splitting of the fibers in the middle of the gauge length and the failure of specimens were sudden.

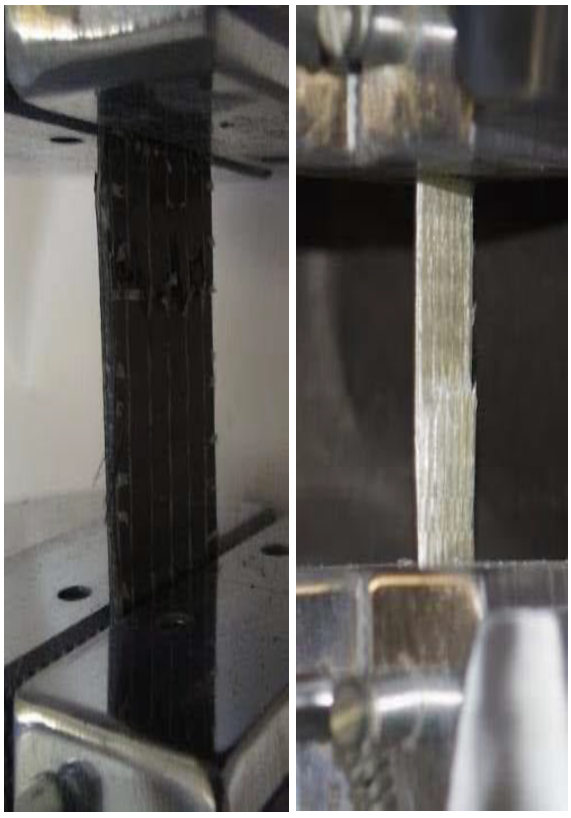

(a) (b)

Fig. 3.26. Failure modes of non-hybrid specimens under compression, (a) C-(CCCC)s or CFRP (b) C-(GGGG)s or GFRP

Stress-strain curves of CFRP specimens show the catastrophic failure after the peak load as depicted in Fig. 3.27(a). A GFRP specimen failed by delamination of fibers after the failure of exterior layers and the failure was catastrophic. In SH specimen C-SH-(CCGG)s, firstly crushing failure of glass fibers were seen, later crushing of carbon fibers was observed, but the time difference between the failure of both fibers was very less, therefore elongation is not seen in stress-strain curves of C-SH-(CCGG)s specimens [see Fig. 3.27(c)]. In case of SH specimens having carbon fibers in the core region, i.e., carbon fibers in between glass fibers, crushing of the glass fibers was seen, further delamination of the carbon fibers was observed. Hybrid specimens in which glass/carbon fibers layers are alternatively dispersed, and glass fibers are at the surface [C-AH-(GCGC)s], kink fracture (diagonal cracking in the thickness direction) of fibers was observed. In another AH specimen C-AH-(CGCG)s, transverse cracking of fibers was observed, which led to the breakage of the specimen into two parts.

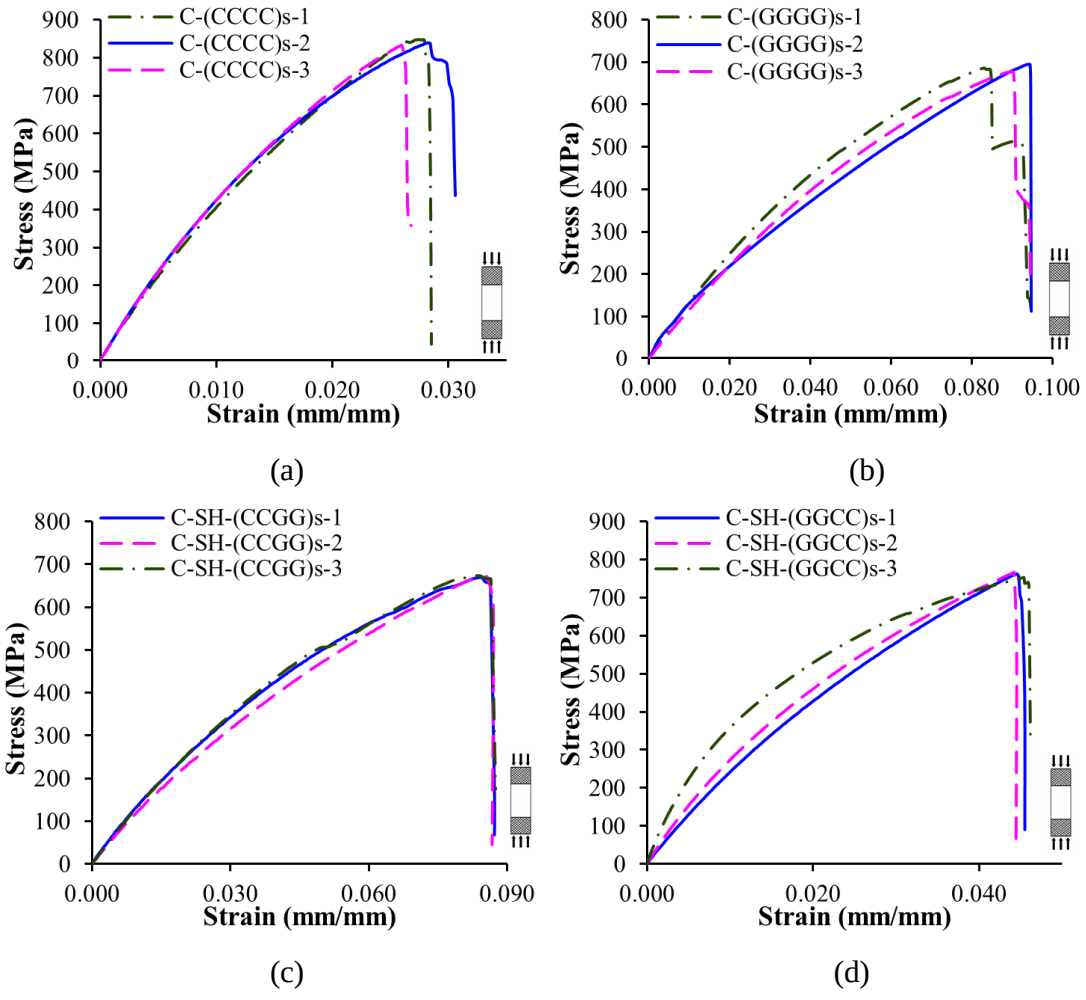

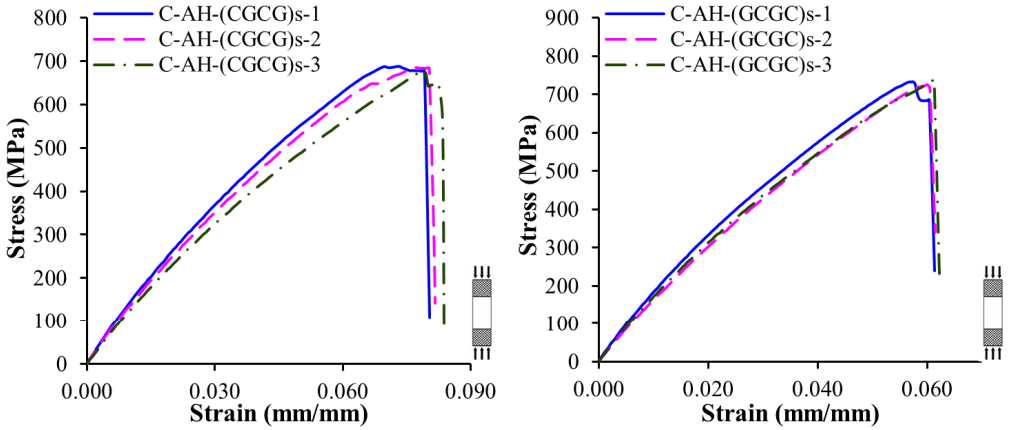

(e) (f)

Fig. 3.27. Stress-strain graphs of plain FRP, sandwich hybrid (SH), and alternate hybrid (AH) compressive specimens: (a) C-$(CCCC)_s$; (b) C-$(GGGG)_s$; (c) C-SH-$(CCGG)_s$; (d) C-SH-$(GGCC)_s$; (e) C-AH-(CGCG)s; (f) C-AH-$(GCGC)_s$

Compressive response of functionally graded specimens is shown in Fig. 3.28. In FH specimen C-FH-$(GC)_s$-I, internal fibers failed before exterior, and the failure was progressive as shown in Fig. 3.28(d). In contrast, other functionally graded hybrid specimens failed catastrophically, and carbon fibers failed earlier than glass fibers. Unlike breakage of C-AH-$(CGCG)_s$ and C-AH-$(GCGC)_s$ specimens at middle, FH specimens failed by cracking of fibers in core region and/or delamination at the surface of the specimen.

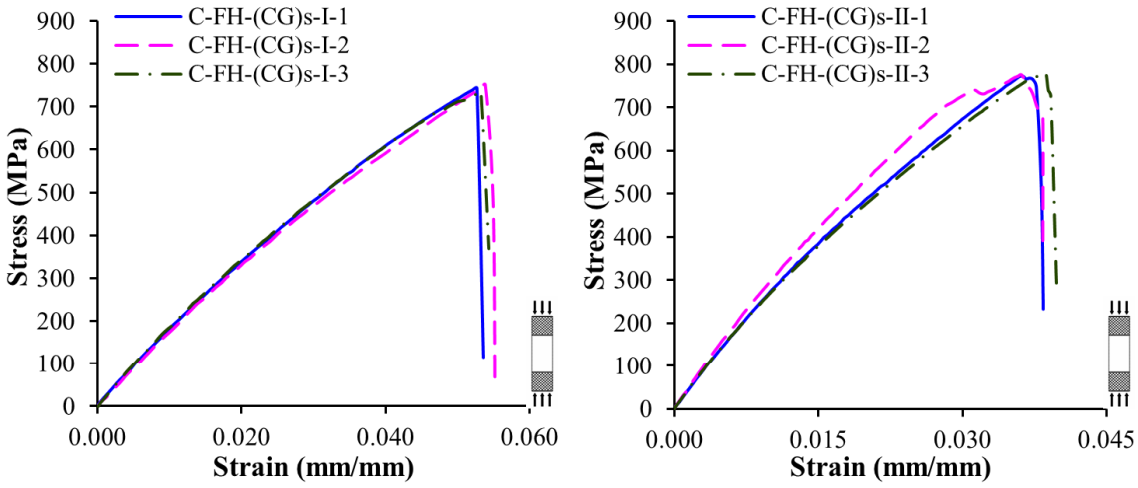

(a) (b)

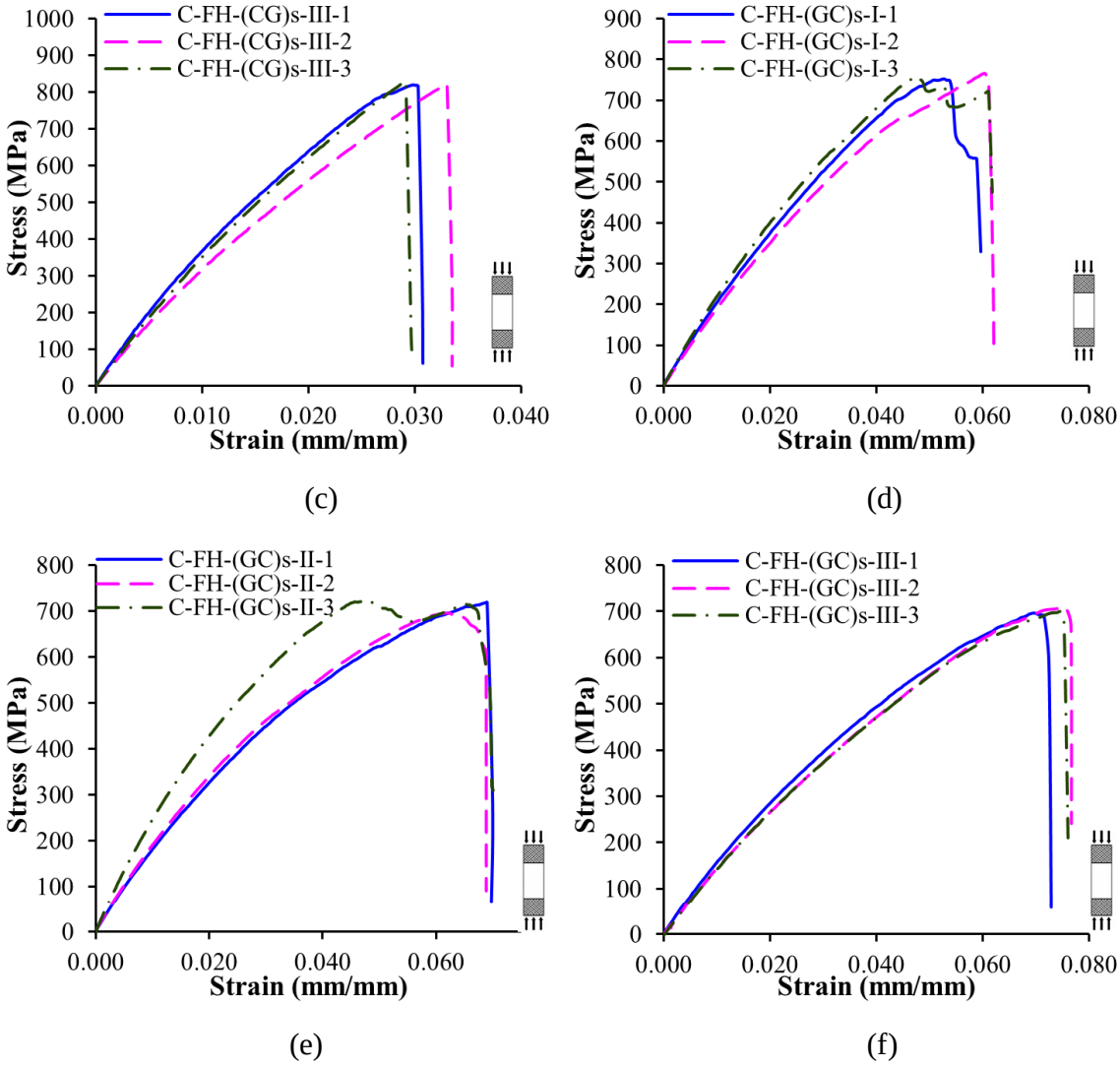

Fig. 3.28. Compressive stress-strain curves of functionally graded hybrid specimens: (a) C-FH-$(CG)_s$-I; (b) C-FH-$(CG)_s$-II; (c) C-FH-$(CG)_s$-III; (d) C-FH-$(GC)_s$-I; (e) C-FH-$(GC)_s$-II; (f) C-FH-$(GC)_s$-III

3.4.2.4. Strength and failure strain

Functionally graded hybrid specimen C-FH-(CG)s-III exhibits higher compressive strength than plain GFRP and SH specimens, while the failure strain of SH composite is higher than plain CFRP composite and FH specimens as shown in Table 3.7. It is noted that with increasing the width of gradation of glass fibers in the core of functionally graded specimens, compressive strength increases. The hybrid effect of the C-FH-(CG)s-III specimen in terms of compressive strength with respect to GFRP specimens is significantly higher than other specimens, i.e., 17%. The SH

specimen C-SH-(CCGG)s has 67% higher failure strain than CFRP specimens and 9% lower failure strain than GFRP specimens. It is also worth noting that hybrid composite having alternate glass and carbon fiber layers have higher compressive strength but the lower failure strain than SH composites. From Table 3.7, it is noted that functionally graded hybrid specimens having glass fibers in core have higher compressive strength except FH-CG-I and lower failure strain than that of the specimens having carbon fiber in core and the same behavior is observed in the sandwich and alternate layers hybrid specimens also. From analytical model, the average compressive strength of hybrid laminate obtained is 754 MPa which is closer to the compressive strength of hybrid laminate obtained from experimental investigation. Hence, the analytical equations used in this study are recommended to determine the compressive strength of the hybrid laminates.

Table 3.7. Mechanical properties such as compressive strength, corresponding failure strain, flexural strength and corresponding flexural modulus

Specimen ID	Compressive strength (MPa)	Failure strain (mm/mm)	Flexural strength (MPa)	Flexural modulus (GPa)
CCCC	840	0.0286	1082	60
GGGG	686	0.0949	703	33
SH-CCGG	671	0.0873	817	71
SH-GGCC	761	0.0454	886	53
AH-CGCG	685	0.0820	931	60
AH-GCGC	731	0.0617	991	59
FH-CG-I	744	0.0544	841	58
FH-CG-II	776	0.0388	792	51
FH-CG-III	824	0.0313	887	48
FH-GC-I	759	0.0611	875	44-
FH-GC-II	713	0.0696	894	56
FH-GC-III	702	0.0752	878	43

3.4.3. Flexural characteristics

3.4.3.1. CFRP laminates

Flexural failure of CFRP specimens was brittle as well as catastrophic as shown in Fig. 3.29(a). The specimens failed suddenly with a sounded crack. The crack occurred along the line of the

loading nose, through which the load was applied, i.e., specimen cracked transverse to the fiber direction. The specimens purely exhibited flexural behavior accompanied by breakage of fibers rather than interlaminar shear. The crack tip was honed in CFRP specimens since it fails suddenly without any plastic deformation. Fig. 3.29(b) shows that the maximum flexural strength of the CFRP specimens is obtained at a temperature of 160^{o}C cured for 1-hour duration and has 6% higher strength than room temperature cured CFRP laminates. Specimens among 80^{o}C and 120^{o}C temperature cure, F0-C080-2 and F0-C120-3 specimens are observed to have a maximum value of flexural strength (see Fig. 3.29(b)). Maximum flexural modulus was obtained in the specimens cured at 120^{o}C temperature for 1-hour curing time and the variations between specimens are presented in Fig. 3.29(c). In comparison with flexural strength, there is significant increase in the flexural modulus, if the specimens are cured at temperature of 120^{o}C for 1-hour. Flexural specimen cured at room temperature attained maximum strain (see Fig. 3.29(d)). Like tensile and compressive longitudinal failure strains, flexural failure strains of temperature cured laminates are also lower than that of room temperature cured laminate. Flexural characteristics normalized with respect to room temperature cured specimen properties depicting the material behavior of CFRP specimens cured at specific temperatures for a certain time period are depicted in Fig. 3.30 for 1 to 3 hours duration. Flexural strength, flexural modulus, and failure strain of the corresponding specimen are shown in Figs. 3.30(a), 3.30(b) and 3.30(c), respectively.

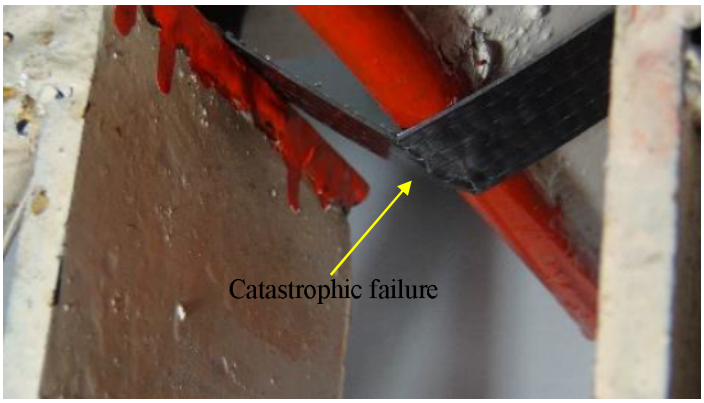

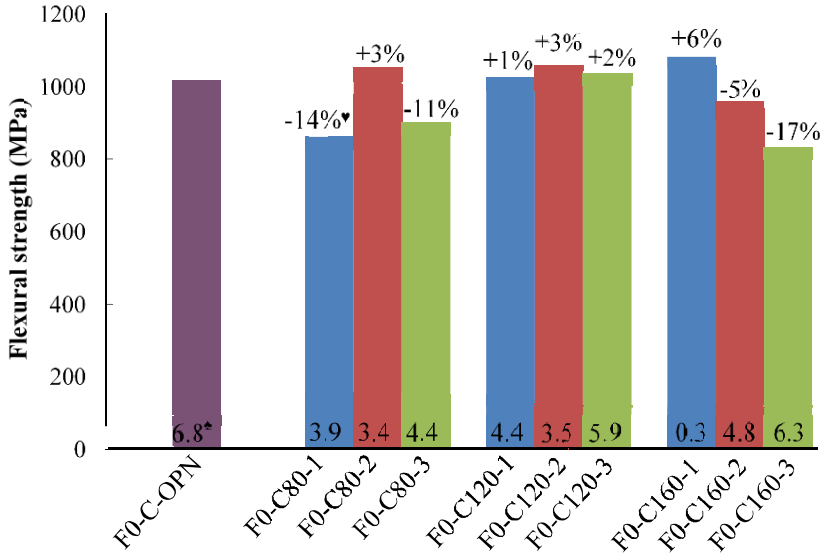

♠Coefficient of variation, ♥Variation w.r.t. room temperature cured specimen (F0-C-OPN)

(b)

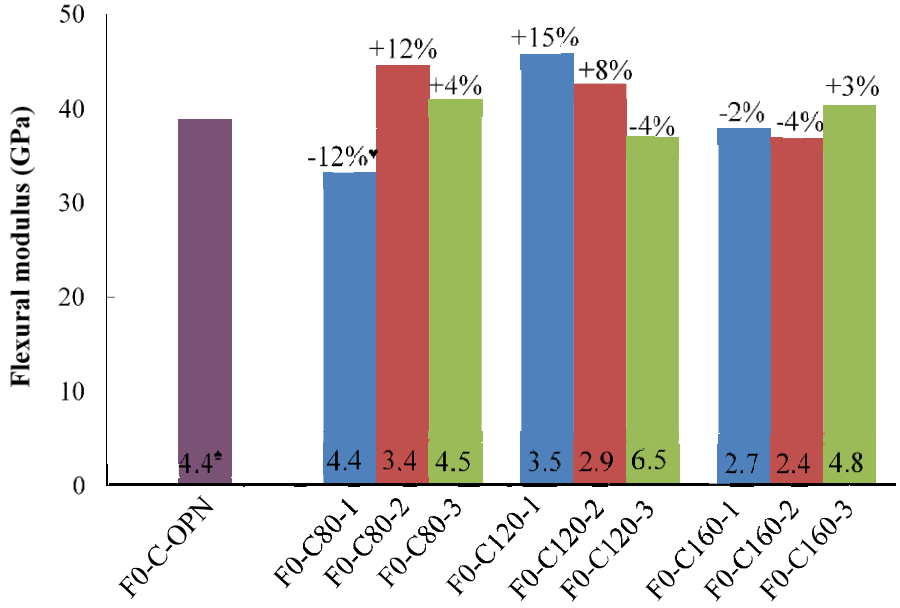

♠Coefficient of variation, ♥Variation w.r.t. room temperature cured specimen (F0-C-OPN).

(c)

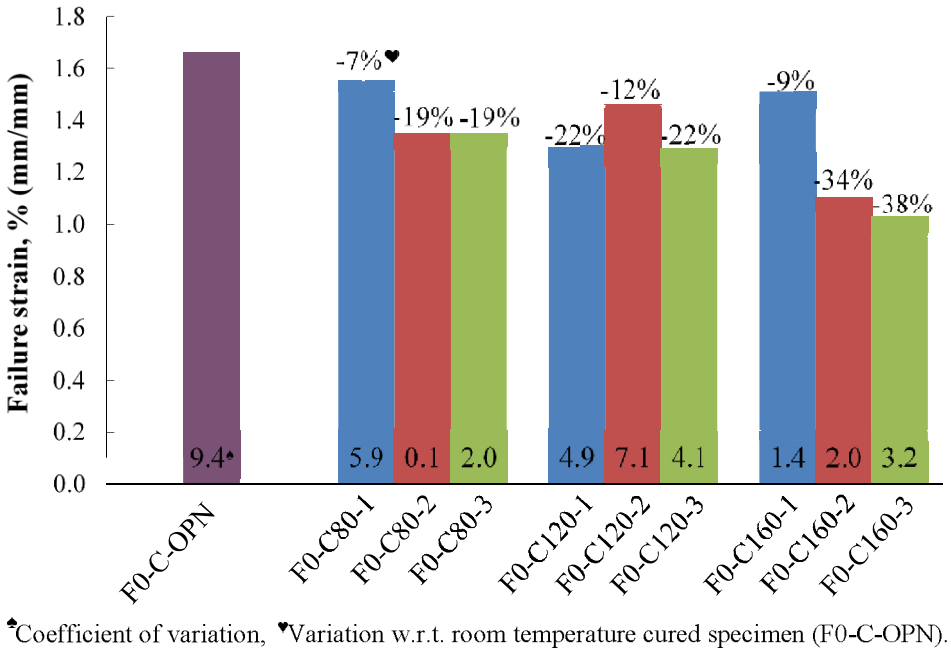

♠Coefficient of variation, ♥Variation w.r.t. room temperature cured specimen (F0-C-OPN).

(d)

Fig. 3.29. Flexure test results of 0^o fiber aligned CFRP specimens: (a) Failure mode, (b) Flexural strength, (c) Flexural modulus, (d) Failure strain.

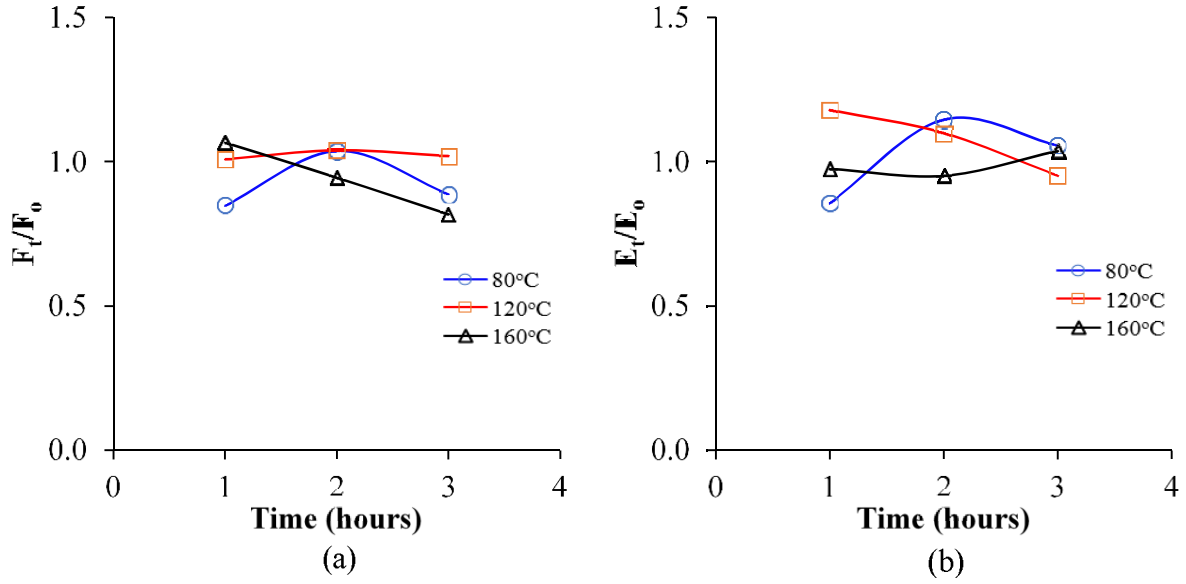

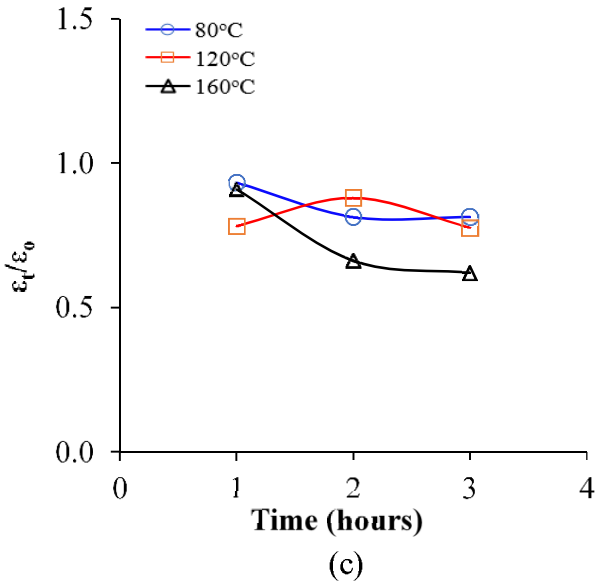

Fig. 3.30. Normalized curves of flexural characteristics of CFRP specimens: (a) Flexural strength of 0^o fiber aligned specimens, (b) Flexural modulus of 0^o fiber aligned specimens, (c) Failure strain of 0^o fiber aligned specimens.

3.4.3.2. GFRP laminates

In three-point bending test of GFRP specimens, ductile bending failure was seen (see Fig. 3.31(a)). During testing, GFRP specimens were able to withstand the load even after the first crack appeared. The specimens underwent plastic deformation as well as progressive failure ahead of the final failure. There were no signs of interlaminar shear failure in these specimens. The crack tip was blunt in case of GFRP specimens due to the plastic deformation. Specimens F0-G160-1 and F0-G120-3 have been observed to have high flexural strength and modulus, respectively (see Figs. 3.31(b) and 3.31(c)). Maximum failure strain was observed for the specimen cured at 120°C for 2-hour curing time which is 19% higher than the room temperature cured specimens. Fig. 3.31(d) shows that there is significant enhancement in failure strain of laminates cured at 120°C temperature for two hours. In the previous sections, it is noted that longitudinal tensile and compressive failure strain of temperature cured GFRP specimens are higher than room temperature cured specimens, but few temperature cured specimens have lower flexural strain in comparison to room temperature curing. It is concluded that in general specimens cured for specific temperature and duration have higher flexural strength and failure strain than room temperature cured specimens. Normalization of flexural characteristics such as flexural strength, flexural

modulus, and failure strain of temperature cured GFRP specimens for various time periods with respect to the room temperature are depicted in Figs. 3.32(a), 3.32(b), and 3.32(c), respectively. It is observed that curing at 160°C for 1 hour is almost equivalent to curing at 120°C for 3 hours for flexural strength, flexural modulus, and flexural failure strain.

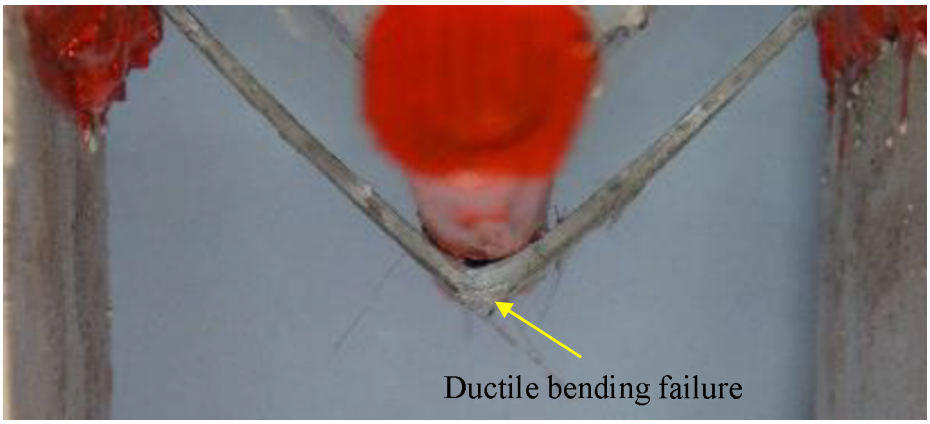

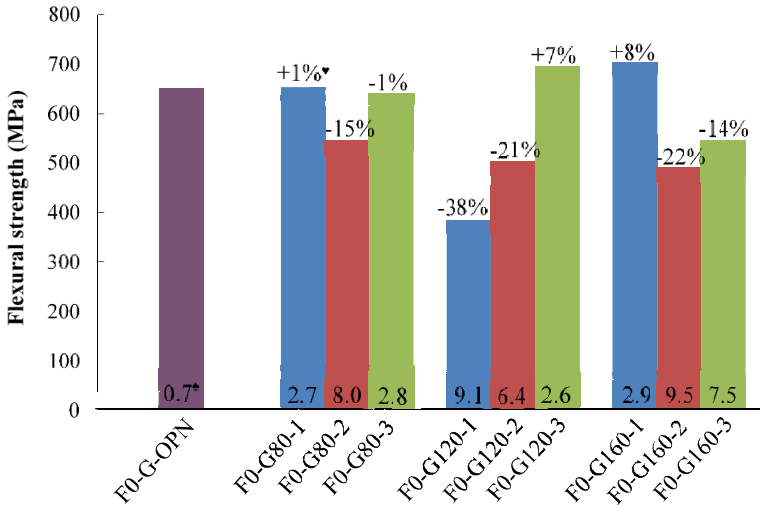

♠Coefficient of variation, ♥Variation w.r.t. room temperature cured specimen (F0-G-OPN).

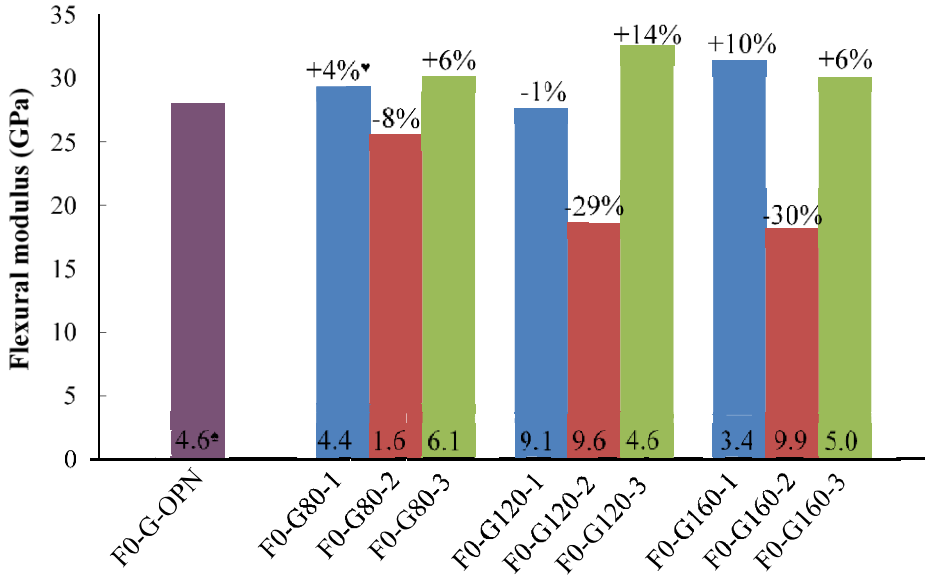

♠Coefficient of variation, ♥Variation w.r.t room temperature cured specimen (F0-G-OPN).

(c)

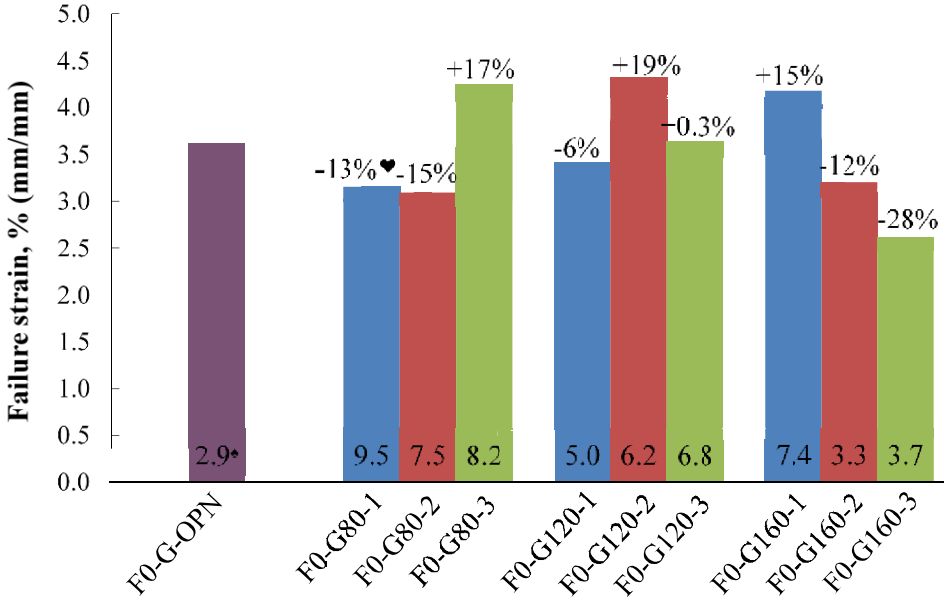

♠Coefficient of variation, ♥Variation w.r.t. room temperature cured specimen (F0-G-OPN).

(d)

Fig. 3.31. Flexure test results of 0° fiber aligned GFRP specimens: (a) Failure mode, (b) Flexural strength, (c) Flexural modulus, (d) Failure strain.

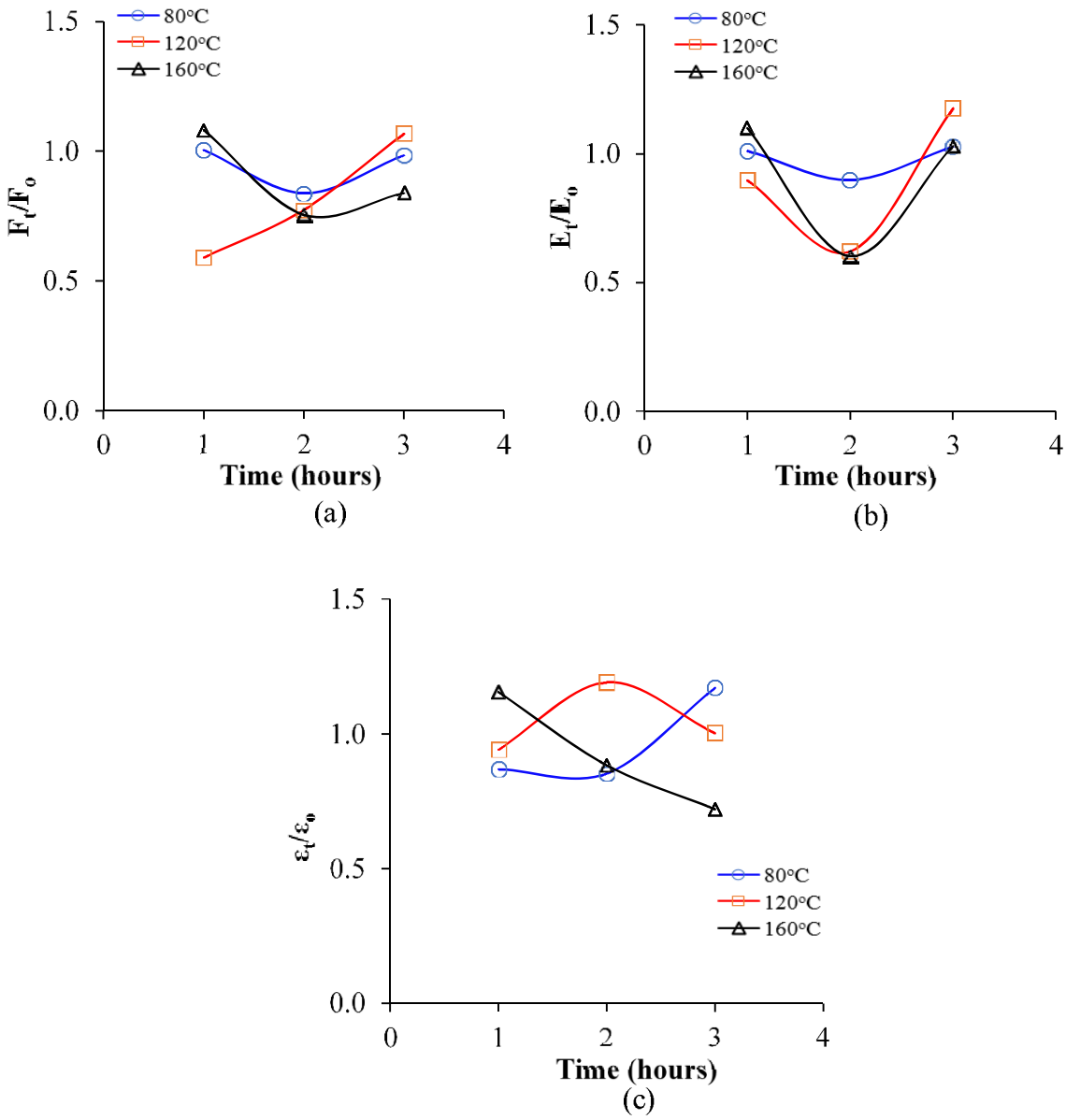

Fig. 3.32. Normalized curves of flexural characteristics of GFRP specimens: (a) Flexural strength of 0^o fiber aligned specimens, (b) Flexural modulus of 0^o fiber aligned specimens, (c) Failure strain of 0^o fiber aligned specimens.

3.4.3.3. Failure modes

Flexural testing of non-hybrid specimens is shown in Fig. 3.33, and load versus deflection responses of the specimens are shown in Figs 3.34 and 3.35. As expected CFRP specimens failed catastrophically and specimens were split in two parts [Fig. 3.33(a)], but there was no delamination

produced in the specimen. In contrast, delamination and flexural cracking were observed in GFRP specimens as shown in Fig. 3.33(b).

(a) (b)

Fig. 3.33. Specimens failed after three-point bending test, (a) F-$(CCCC)_s$ (b) F-$(GGGG)_s$

Moreover, in comparison with load-deflection curves of CFRP specimens, GFRP specimens show progressive failure and the ultimate failure strain is high. The SH specimens having glass fibers at exterior and carbon fibers in core, i.e., F-SH-(GGCC)s failed by combination of delamination of carbon fibers and tensile cracking of glass fibers at the tension side. On the other hand, in SH specimens having carbon fibers at exterior and glass fibers at core [F-SH-(CCGG)s], firstly transverse cracks were observed in the exterior layers (carbon fibers), later glass fibers failed, as a consequence of this, high failure strain is observed in the specimens. Specimens having alternate layers of glass and carbon fibers [F-AH-(CGCG)s and F-AH-(GCGC)s], failed in ductile with delamination and rupture of fibers. Flexural testing of FH specimens having glass fibers at the exterior surface shows that very fine cracking of fibers was observed at the tension face of the specimens and delamination was noted in between the layers of carbon fibers. While in the case of FH specimens having carbon fibers at the exterior layer, kink fractures were seen in the carbon fiber layer. In Fig. 3.35, load-deflection curves of the FH specimens show the progressive failure after peak load, which is due to the functional gradation of fibers, as a result, fibers failed layer-wise. It is worthwhile to mention that due to gradual dispersion of fibers, progressive failure observed in FH specimens, which is the major advantage of FH laminate, which is missing in most of SH specimens (Fig. 3.34).

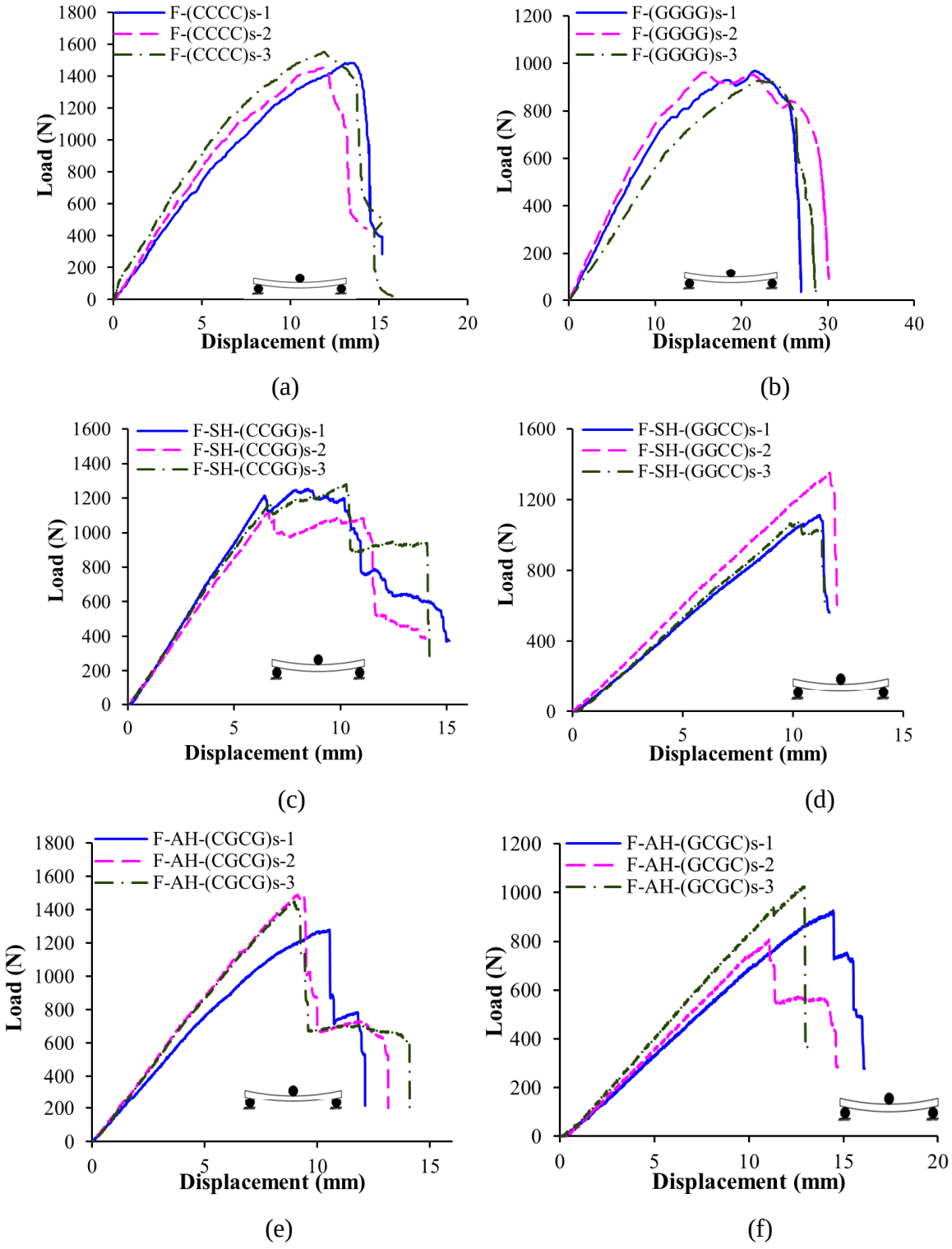

Fig. 3.34. Load-displacement diagrams of plain FRP and sandwich hybrid flexural specimens: **(a)** F-$(CCCC)_s$ **(b)** F-$(GGGG)_s$ **(c)** F-SH-$(CCGG)_s$; **(d)** F-SH-$(GGCC)_s$; **(e)** F-AH-$(CGCG)_s$; **(f)** F-AH-$(GCGC)_s$

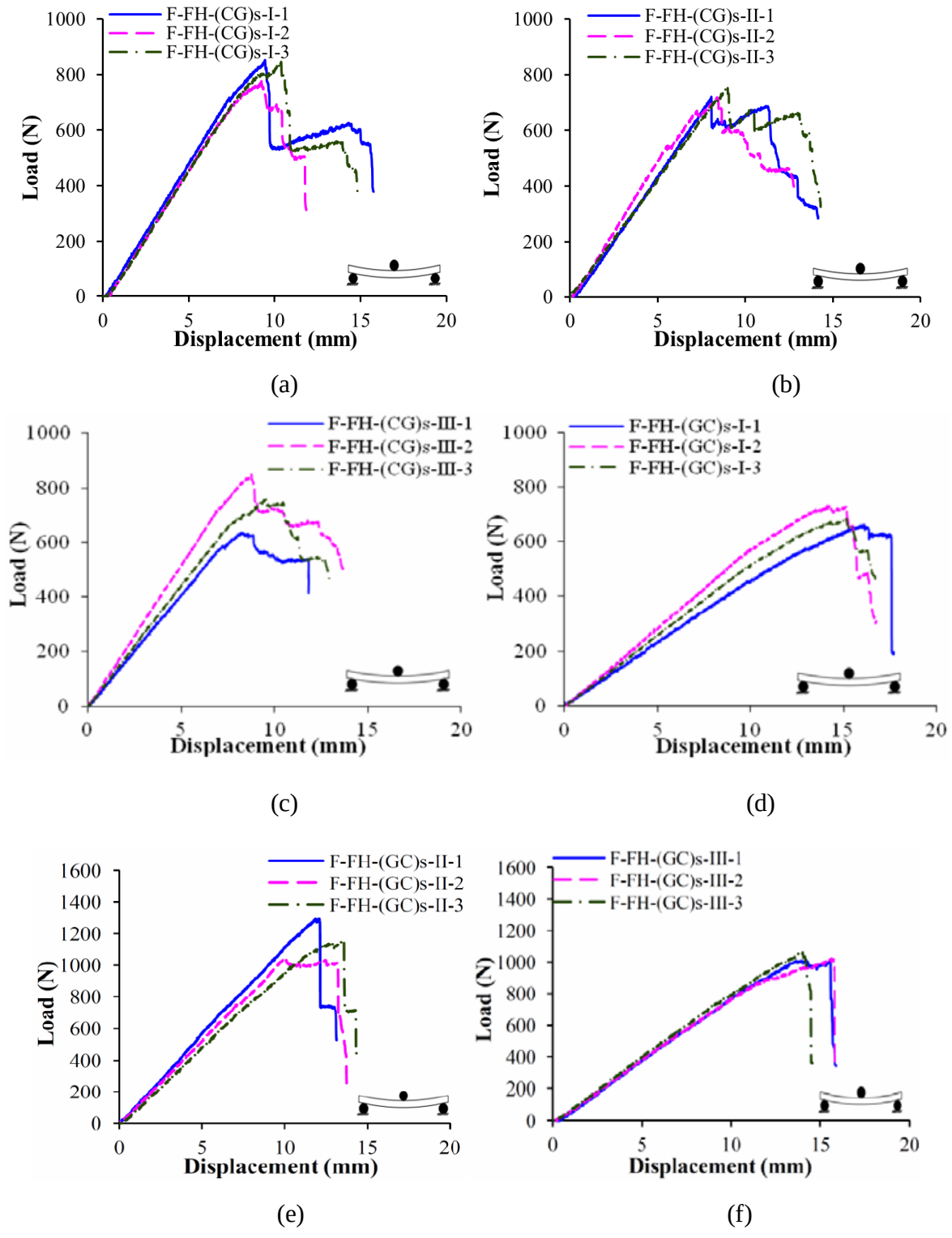

Fig. 3.35. Load-displacement diagrams of flexural functionally graded hybrid specimens: (a) F-FH-$(CG)_s$-I; (b) F-FH-$(CG)_s$-II; (c) F-FH-$(CG)_s$-III; (d) F-FH-$(GC)_s$-I; (e) F-FH-$(GC)_s$-II; (f) F-FH-$(GC)_s$-III

3.4.3.4. Strength, stiffness and failure strain

In Fig. 3.36, bar charts show the comparison of flexural strength and modulus of the hybrid laminates with CFRP and GFRP specimens. Among all hybrid specimens, alternate layers of glass and carbon fiber hybrid specimens have high flexural strength than GFRP, sandwich hybrid and functionally graded hybrid specimens. Hence, it is stated that specimens in which carbon fibers surrounding each layer of glass fibers, i.e., alternate layers of glass and carbon fibers is more effective in enhancing the strength of the laminate than that of glass fibers sandwiched in between carbon fibers. It is worth to mention that specimens having glass fibers sandwiched in between carbon fibers (F-SH-$(CCGG)_s$) have higher stiffness than all hybrid and non-hybrid specimens. Stiffness of both alternate layers of hybrid specimens having different layup is also same and is equivalent to CFRP specimens. Therefore, it is concluded that alternate layers hybrid is most effective hybrid because its strength and stiffness is equivalent to CFRP specimens. Among all functionally graded hybrid laminates, specimen F-FH-$(GC)_s$-II, has higher strength and stiffness than all other functionally graded hybrid laminates.

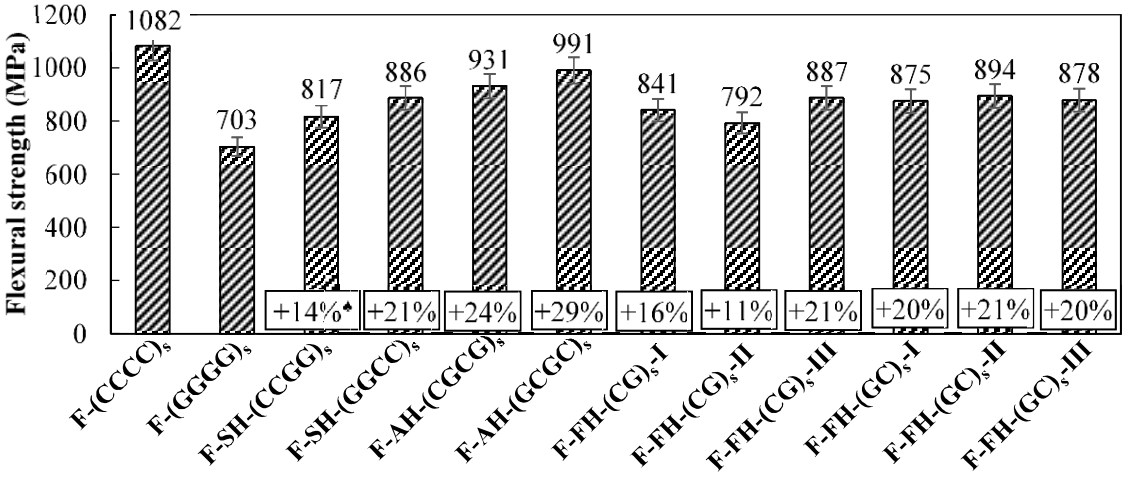

♥Hybrid effect w.r.t. GFRP

(a)

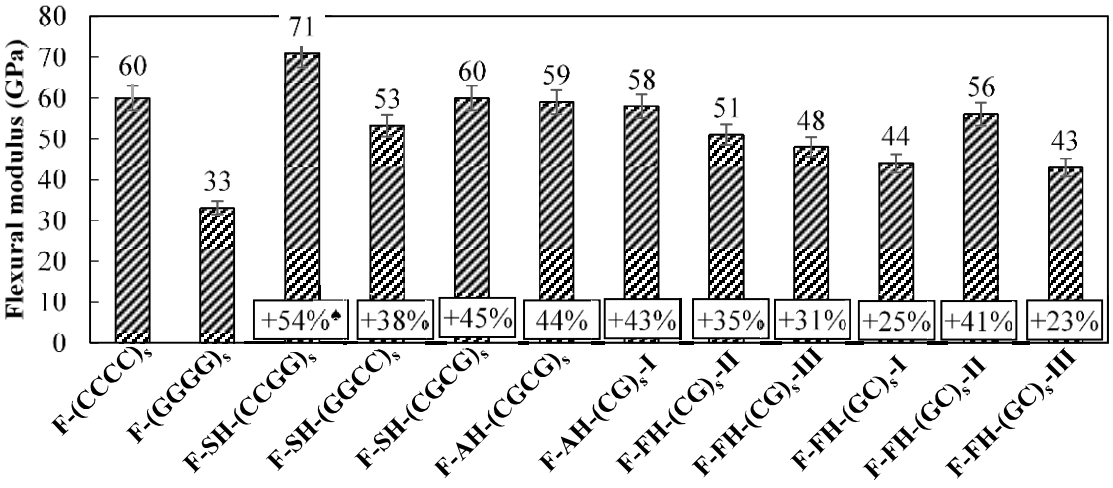

♠Hybrid effect w.r.t. GFRP

(b)

Fig. 3.36. Comparison of flexural properties: (a) Flexural strength; (b) Flexural modulus

3.5. Concluding remarks

In this study, influence of curing temperature such as 80°C, 120°C and 160°C and curing duration (1, 2 or 3 hours) on tensile, compressive, shear and flexural strengths, stiffness and failure strain of plain and hybrid specimens are examined experimentally. Also, a a novel functionally graded hybrid laminate made of carbon and glass fibers is fabricated. Tensile, compressive, and flexural responses of the functionally graded hybrid laminate are compared with that of conventional sandwich and alternate layers hybrid laminates. The existence of positive or negative hybrid effect in hybrid specimens with respect to strength and stiffness predicted from the ROM (Rule of Mixtures) is demonstrated. From this study, the following concluding remarks are made.

1. CFRP specimens aligned in 0° fiber direction cured at 80°C temperature for 3-hour duration, achieved maximum tensile strength and stiffness. Moreover, specimen cured at 160°C temperature for about two hours, has transverse tensile strength equivalent to room temperature cured specimen while maximum stiffness is obtained at 80°C for 1-hour duration which is higher than that of room temperature cured specimens.
2. GFRP 0° fiber aligned specimens cured at 80°C for 3-hour duration is predominant in tensile strength while stiffness is dominant in case of 120°C temperature cured specimens for 3-hour duration. For 90° fiber aligned GFRP tensile specimens, tensile strength is high for 160°C

temperature cured specimens for 1-hour duration, while stiffness is dominant at 160°C temperature curing for about three hours.

3. Shear modulus of CFRP laminates decreases, if specimens are cured at elevated temperature. In case of GFRP laminates, shear modulus depends upon the temperature and duration of curing. The laminate which is cured for three hours at temperature of 160°C gives the highest shear modulus which is 27% higher than that of room temperature cured specimens.
4. CFRP laminate cured at 80°C temperature for 3-hour curing duration has higher longitudinal compressive strength than that of room temperature cured specimen, while the maximum transverse compressive strength of CFRP laminates can be obtained if laminate is cured at 160°C temperature for two hours.
5. Longitudinal and transverse compressive strength of elevated temperature cured GFRP laminates is higher than laminates cured at room temperature. The laminates cured at temperature of 80°C for 1-hour have higher strength than that of room temperature or other oven cured laminates.
6. Tensile and compressive failure strains of GFRP laminates are higher at elevated temperature than at room temperature, while the longitudinal failure strains of CFRP laminates is lower at elevated temperature. The transverse compressive failure strain of CFRP laminates at elevated temperature is higher than that at room temperature, while the transverse tensile failure strain depends upon temperature and curing time.
7. Flexural strength of specimens cured at 160°C for 1-hour duration is predominant for both CFRP and GFRP specimens. Maximum flexural modulus in CFRP specimens is obtained at 120°C temperature for 1-hour curing while in the case of GFRP specimens, maximum modulus is obtained at 120°C temperature for 3-hour curing.
8. Flexural failure strain of temperature cured CFRP specimens is lower than room temperature cured CFRP specimens. The flexural failure strain of GFRP laminates is higher for temperature curing than room temperature curing for specific temperature and curing duration such as 80°C temperature for three hours, 120°C for two hours and 160°C for one hour. Maximum flexural failure strain of GFRP laminate is obtained at curing temperature of 160°C for 1-hour duration.
9. Functionally graded hybrid laminate (FH-$(CG)_s$-II) specimen has highest tensile strength amongst all sandwich and alternate layer hybrid specimens. The tensile strength of this specimen shows the existence of positive hybrid effect since its strength is higher than plain

GFRP laminate. Alongwith, modulus of elasticity of functionally graded hybrid specimen (FH-$(CG)_s$-I) is higher than all specimens including plain CFRP and GFRP.

10. Functionally graded hybrid specimens also show more progressive failure than sandwich and alternate layer hybrid specimens in tension. Functional gradation of carbon fiber around glass fibers, i.e., glass fibers in the core, is proved to be better than functional gradation of glass fibers around carbon fibers, because of its higher strength and stiffness.
11. The maximum total energy and inelastic energy have been absorbed by functionally graded hybrid specimen T-FH-$(GC)_s$-III. Therefore, this specimen T-FH-$(GC)_s$-III have the highest ductility. Furthermore, the highest elastic energy was obtained by sandwich hybrid specimen T-SH-$(GGCC)_s$ in which glass fiber acts as the surface layer.
12. Functionally graded hybrid laminate (C-FH-$(CG)_s$-III) has peak compressive strength among the sandwich and alternate layer hybrid laminates. Nevertheless, these specimens exhibit less compressive strength when compared with plain CFRP specimens. Sandwich hybrid laminate (SH-$(CCGG)_s$) exhibits highest failure strain than all other hybrid laminates.
13. Flexural strength of the alternative layer hybrid specimen (F-AH-$(GCGC)_s$) is higher than the sandwich and functionally graded hybrid specimens. Moreover, functionally graded hybrid specimen (F-FH-$(GC)_s$-II) has 10% lesser flexural strength than F-AH-$(GCGC)_s$ specimen and 18% lower strength than CFRP specimens. Flexural modulus of sandwich hybrid specimens is similar to the CFRP specimens, while the flexural modulus of F-FH-$(GC)_s$-II is 7% lesser than that of CFRP.
14. The functionally graded hybrid specimens proved to be better in the uniaxial tension and compression, while its flexural stiffness is equivalent to the stiffness of CFRP. Therefore, it is concluded that functionally graded hybrid can replace conventional hybrids such as sandwich and alternate layers hybrids.
15. The tensile, and compressive strengths of FH-$(CG)_s$-I specimen obtained from analytical equations are closer to that obtained from experimental tests. FH-$(CG)_s$-III specimen has 2.8% higher experimental elastic modulus than the value obtained from analytical equation which is considered as a minor deviation. Hence, it's been stated that the analytical equations used in this study can be used to determine the strength and stiffness of the functionally graded hybrid specimens.